T.C. DOĞUŞ UNIVERSITY

GRADUATE SCHOOL OF SCIENCE ENGINEERING AND TECHNOLOGY

DEPARTMENT OF ELECTRONICS AND COMMUNICATIONS ENGINNEERING

INVESTIGATIONS ON THE EFFECTS OF FOURWAVE-MIXING IN DWDM FIBER CHANNELS

M.Sc. THESIS

Onur ERKAN

Thesis Advisor:

Prof.Dr. Ercan TOPUZ

İSTANBUL, February 2013

T.C. DOĞUŞ ÜNİVERSİTESİ

FEN BİLİMLERİ ENSTİTÜSÜ

ELEKTRONİK VE HABERLEŞME MÜHENDİSLİĞİ BÖLÜMÜ

INVESTIGATIONS ON THE EFFECTS OF FOURWAVE-MIXING IN DWDM FIBER CHANNELS

M.Sc. THESIS

Onur ERKAN

200892001

Thesis Advisor:

Prof.Dr. Ercan TOPUZ

İSTANBUL, February 2013

FOREWORD

I would like to thank the all people who supported me carrying out this work, without their help and support this thesis would not have been possible.

Firstly, I like to extend my gratitude to my academic supervisor Prof. Dr. Ercan Topuz for accepting me as Ms candidate. Especially I want to thank for his encouragements and guidance throughout the thesis. His deep insights and expertises in fiber optics have made this work possible.

I want to thank my wife Feyza Erkan for her support and patience during thesis with an everlasting positive energy and motivation. I would also like to thank my parents for their unconditional support during the time I studied.

Finally I would like to express my gratitude to Technology Division of Vodafone Turkey for the opportunity to write my thesis on such a related topic with industrial focus area of fiber optics communications.

İstanbul, February 2013 Onur ERKAN

TABLE OF CONTENTS

INVESTIGATIONS ON THE EFFECTS OF FOURWAVE-MIXING IN DWDM FIBER CHANNELS

ABSTRACT

Optical fiber cables have become ideal for achieving the challenge of reaching high speed data rates and terabit transmission, due to its low attenuation characteristics and high bandwidth capability such as 50 THz. Multiplexing of numerous channels on the same fibre requires higher transmit power or sufficiently lower fibre losses to utilize the available bandwidth having high bit rate with a span of thousands of kilometer.

It is required to increase the number of optical channels in dense WDM systems in order to meet the extreme capacity demands on data transmission networks. This necessity of increment in number of channels can be provided only with small channel spacing. In order to reach required amount of signal channels, new frequency standards such as 25 GHz and 12.5 GHz were recently specified by ITU. In such narrower channel spacing with large number of WDM channels, the non-linear effects of the optical fibre can induce serious system impairments. In modern WDM systems, the primary nonlinear effects are cross phase modulation (XPM), and the four-wave mixing (FWM). The FWM characteristics are especially related to frequency allocation of channels. Throughout this thesis, we will be mainly dealing with the FWM impairments.

The occurrence of FWM depends on several factors, such as frequency spacing between channels, the input power per channel, the dispersion characteristics of the optical fiber, and the distance along which the channels interact.

Four wave mixing results from changes in the refractive index with optical power called optical Kerr effect. In FWM, two co-propagating waves produce two new optical sideband waves at different frequencies. The generation of these beat signals which fall into original signal wavelengths causes a channel energy loss, which induces a crosstalk effect. In long haul transmission links, the deployment of optical amplifiers makes the problem even worse, as not only the transmitted signal is amplified, but also the generated FWM products, which mix again with the signals, causing new products. Also when intense incident signal power launched into a fiber, linearity of optical response is lost. Moreover, in the usage of dispersion-shifted fibers (DSF), the FWM mechanism is enhanced, due to a depletion of the phase mismatch associated to the fiber's chromatic dispersion. In consequence, the detected signal power will fluctuate considerably.

Numerous techniques have been proposed to minimize the detrimental limiting effects of FWM such as: the spectral allocation of the channels, the spectral assignment of the channels as far as possible from the zero-dispersion wavelength (λ_{ZD}), and the spectral distribution of the unequally spaced channels, which requires a complex system design.

In this study, the impact of the channel spacing (positioning of the DWDM channels), phase mismatching, changing of channel input power and fiber length on FWM efficiency were analyzed based on represented algorithm. For various types of fibers such as G.652

(Single- Mode Fiber - SMF), G.653 (Dispersion-Shifted Fiber - DSF), and G.655 (Non-Zero Dispersion-Shifted Fiber - NZDSF) compliant fibers, considering the DWDM grids suggested by the ITU-T Recommendations G.692, and G.694.1, with uniform channel spacing of 100, 50, 25, and 12.5 GHz were compared with simulations. Split Step Fourier Method (SSFM) numerical technique has been used to model nonlinear Schrödinger (NLS) equation in order to investigate pulse propagation in optical fibers.

DALGA BOYU BÖLMELİ ÇOĞULLAMA SİISTEMLERİNİN FİBER KANALLARINDA DÖRT DALGA-KARIŞIMI ETKİLERİNİN İNCELENMESİ

ÖZET

Fiber optik kablolar, düşük zayıflama özellikleri ve 50 THz gibi yüksek bant genişliği sağlayabilen profilleri sayesinde yüksek hızlı verilerin aktarımına ulaşmak için ideal hale gelmiştir. Aynı fiber üzerinden, binlerce kilometrelik mesafelerde yüksek bit hızı ile mevcut bant genişliği kullanmak için çok sayıda kanalın çoğullanması, yüksek iletim gücü yada kaybı yeterince düşük fiber gerektirir.

Veri iletimi şebekelerinde artan kapasite taleplerini karşılamak amacıyla yoğun dalga boyu bölmeli çoğullama (WDM) sistemlerinde optik kanal sayısını artırmak gerekmiştir. Gerekli olan bu kanal sayısı artışı sadece kanal aralığı küçük tutularak sağlanabilir. İstenen sayıda sinyal kanalına ulaşabilmek için uluslar arası telekomünikasyon kurumu (ITU) tarafından belirlenen son frekans aralıkları olan 25 GHz ve 12.5 GHz frekanslar kullanılmaktadır. Bu denli yakın kanal boşlukları kullanılarak elde edilen WDM sinyalleri, optik fiberin doğrusal olmayan etkileri sebebiyle ciddi sistem bozukluklarına neden olabilir. Modern WDM sistemlerinde doğrusal olmayan etkilerin başlıcaları Çapraz-Faz Modülasyonu (XPM) ve Dört-Dalga Karışımı (FWM), sistem performansını sınırlandırmaktadır. FWM etkisinin karakteristiği özellikle kanalların frekans düzlemindeki tahsisi ile ilişkilidir. Bu tez boyunca, FWM bozuklukları ve etkileri ele alınıp incelenmiştir.

FWM oluşumu; kanallar arası frekans aralığı, kanal başına giriş gücü, optik fiberin dispersiyon özellikleri ve kanalların aldığı mesafe boyunca birbirleri ile etkileşimi gibi birçok faktöre bağlıdır.

Dört dalga karışımı, "Optik Kerr Etkisi" adı verilen fiber kırılma indisinin optik güç ile değişiminden gelmektedir. FWM etkisinde, eş yayılan iki dalga farklı frekanslarda iki yeni optik yan dalga üretmektedir. Bu bozucu yan dalga ürünlerinin orijinal sinyal kanalları üzerinde oluşması sonucu enerji kaybı meydana gelmekte ve çapraz karışım etkisine sebep olmaktadır. Uzun mesafeli veri iletim hatlarında, optik kuvvetlendiricilerin kullanılması; problemi daha da ciddileştirmekte olup iletilecek ana sinyal ile beraber FWM ürünü sinyallerin de kuvvetlendirilmesine, karışıma sebep olacak yeni ürünler doğmasına sebep olmaktadır. Ayrıca fibere yoğun bir giriş sinyali uygulandığında optik doğrusallık bozulmaktadır. Buna ilaveten Dispersiyonu Kaydırılmış Fiber (DSF) kullanılması durumunda, fiberin kromatik dispersiyonu ile ilişkili olarak faz uyumsuzluğunun azalması sonucu FWM etkisi gelişir. Bunun sonucu olarak elde edilen edilen sinyal gücü önemli ölçüde dalgalanır.

FWM ve sınırlayıcı etkilerinin minimize edilmesi için sayısız teknik geliştirilmiştir. Kanalların spektral dağılımı, sıfır-dispersiyon dalga boyundan (λ_{ZD}) mümkün olan en uzak

mesafede kanalların seçimi ve eşit olmayan bir spektral dağılım, karmaşık bir sistem tasarımı gerektiren tekniklerdir.

Bu tez çalışmasında, kanal aralığının etkisi (DWDM kanal konumlandırması), faz uyuşmazlığı, kanal giriş gücünün ve fiber uzunluğunun değişiminin FWM verimliliği üzerinde etkisi sunulan algoritma kullanılarak analiz edilmiştir. ITU-T G.692 ve G.694.1 DWDM kanal dağılım standardları olan 100, 50, 25 ve 12.5 GHz kanal aralıkları ile fiber standartları olan G.652 basamak-indisli tek modlu optik fiber (step-index, SMF), G.653 dispersiyonu kaydırılmış fiber (DSF) ve G.655 sıfırlanmamış dispersiyonu kaydırılmış fiber (NZDSF) türleri simülasyonlarda karşılaştırılmıştır. Simülasyonlarda optik fiberin darbe yayılımını sayısal teknik ile araştırmak amacıyla parçalı adım Fourier metodu (SSFM) ile doğrusal olmayan Schrödinger (NLS) denklemi çözülmektedir.

LIST OF FIGURES

Page

LIST OF TABLES

Page

1. INTRODUCTION

1.1 Background and Problem Definition

The rapid increase of worldwide communication, internet and multimedia demands has led to an explosive growth of high speed digital communications. Throughout the latter quarter of the 20th century fiber optics has been indispensable in facilitating this extraordinary load [1].

Modern commercial fiber optic systems are capable of transmitting hundreds of gigabits-per-second, with experimental systems demonstrating terabit capability [2]. Contemporary optical fibers have a bandwidth in excess of 30 terahertz [3]. While the fiber channel may be capable of transmitting terabit-per-second (Tb/s) data rates, no current single electrical communication system can reach this capacity. The electrical transmitters and receivers on either end of a fiber channel are subject to technological constraints currently which limit their speeds at about 40 Gb/s [4].

Communication systems overcame the electronic limitations with the invention of low-loss optical fibers and wavelength division multiplexing (WDM) thereby resulting in an increment in the transmission capacities [3]**.**

In WDM systems, the available bandwidth is divided into separate channels with each channel carrying one signal. The data rate of each channel frequently limited to 10 Gb/s, but total data rate of all channels are much higher [2]. In order to increase the transmission capacity of WDM optical system, transmission data rate per wavelength has been increased as well as the number of wavelengths.

However, there are two different transmission issues which are limiting factors in long-haul WDM systems: dispersion and fiber nonlinearities.

In terms of the high data rate transmission, the chromatic dispersion (CD) and polarization-mode dispersion (PMD) are typically major obstacles which result in much larger penalties than the nonlinearity of optical fiber. Thus, nonlinear effects were usually neglected prior to the 1990's. With the improvement of dispersion shifted fibers (DSF), dispersion compensating fibers (DCF) and the other dispersion management techniques, the limiting problem of CD has been mitigated [5,6].

As data rates have continued to increase the number of wavelengths the number of wavelengths also increased. Decreasing channel spacing in WDM systems led to limitations due to nonlinearities such as four-wave mixing (FWM) and cross-phase modulation (XPM).

In order to establish communications over long-haul networks the power losses are compansated by using erbium-doped single mode fiber amplifier (EDFA) at about every 50 km in WDM transmission systems.

Although EDFAs make the high optical power levels available in WDM systems, they also led to a more vulnerable system performance by increasing nonlinear effects [7,8]. This leads to interference, distortion, and excess attenuation of the transmitted signals and results in system degradations. As a result, fiber nonlinearities emerged as the most serious limiting factor.

The origin of nonlinearities arise from the variation of the refractive index in an optical fiber that is related to the intensity of the optical signal. This detrimental effect becomes more significant when high aggregate power is launched, even if the individual power of each channel may be below the level needed to produce nonlinearities. The combination of high total optical power and large number of channels at narrower spaced wavelengths leads to the formation of many unwanted components. Hence, four-wave mixing seems to be the most harmful impairment in dense wavelength division multiplexing (DWDM) systems [9-11].

1.2 Introduction to Optical Fibers in Communication Systems

An optical fiber is a dielectric waveguide consisting a core region which has a higher refractive index surrounded by a cladding layer that has lower refractive index material. This type of fiber is called *step-index* fiber. This refractive index difference ensures that the propagating signal power is contained predominantly within the core region which has a higher refractive index. For propagation, the angle of incidence of the propagating light should be smaller than the critical angle at the boundary waveguide. For core region with a refractive index n_c , and for the cladding region with a refractive index n_{cl}, the critical angle can be expressed as

$$\phi_c = \arcsin\left(\frac{n_{cl}}{n_c}\right) \tag{1.1}$$

Another parameter used to characterize an optical fiber is *Numerical Aperture* (N.A.). Numerical aperture is the maximum angle that light can be accumulated into a fiber from its end faces and can be calculated with Snell-law:

$$NA = \sin(\theta_1) = \sqrt{n_c^2 - n_{cl}^2} \tag{1.2}$$

where refractive index of environment is taken as "1" considering incidence from air.

As opposed to step-index fibers, the graded-index fibers have a refractive index profile which has its highest value on the axis and decreases monotonically towards the index of the cladding region. Figure 1.1 shows schematically the index profile and the cross section for the two kinds of fibers.

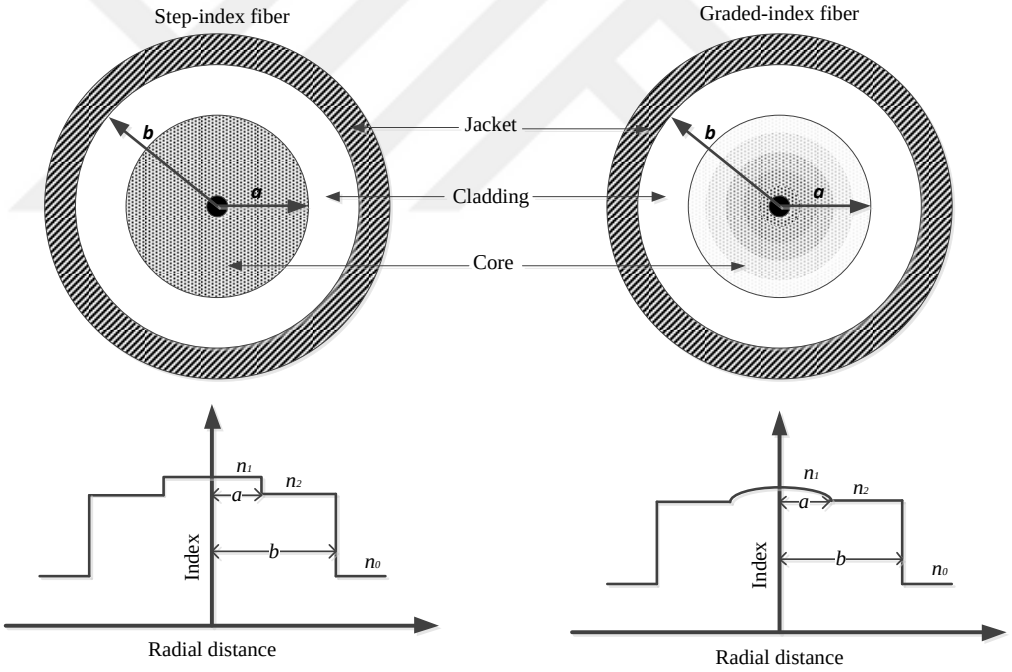

Figure 1.1: Cross section and refractive-index profile for step-index and graded-index fibers [2].

The normalized frequency which is denoted as V determines the number of modes supported by an optical fiber and can be expressed as

$$V = k_0 a (n_c^2 - n_{cl}^2)^{1/2} \tag{1.3}$$

where $k_0 = 2\pi/\lambda$, α is the core radius, and λ is the wavelength of the light. It is observed that the *V* parameter depends on the geometry of fiber and the core-cladding index difference. Industrial fibers are designed to support only one mode that can be satisfied by the *V*<2.405 condition. A step-index fiber which satisfies this condition is referred as *Single-mode fiber(SMF).* In this thesis, only single mode fibers are investigated with different classification of ITU such as G.652, G.653, G.655 fibers. Fiber modes will be explained in more detail in the following chapter.

1.3 WDM Optical Fiber Communication Systems

A standard communication system consists of basic components like multiplexer, demultiplexer, signal source, receiver and carrier medium. In order to use the system in full capacity, a new technique is developed through the simultaneous multiplexing of each channel. Time division multiplexing (TDM) and Frequency division multiplexing (FDM) are two main multiplexing schemes which use time domain and frequency domain respectively. In practice, these two multiplexing techniques can be used both in electrical domain and optical domain. Due to the limitations imposed by electronic components, transmission of multiple channels over same fiber provided a simple way for exploiting the large bandwidth offered by optical fibers. Development of such system corresponds to optical carriers at different wavelengths, which is called Wavelength Division Multiplexing (WDM) [2].

Wavelength division multiplexing (WDM) is a technology used to combine and split two or more optical signals of different optical center wavelengths in a fiber. This technique allows fiber capacity to be expanded in the frequency domain from one channel to more than 100 channels.

The WDM channel wavelength assignment is an industry standard defined in International Tele-communications Union (ITU-T) recommendation (See Appendix-G).

In a typical WDM system (Figure 1.2), bit sequence is modulated in transmitters through optical carriers each at a different wavelength i.e., λ_1 … λ_N with a specific modulation format. Optical bandpass filtering and combining of the individual wavelength signals are performed in multiplexer level. The demultiplexer coupler separates the combined signals

through their corresponding channel ports. Basic WDMs are transparent to all optical protocols such as SONET, SDH, GigE, 10GigE, etc. They are also transparent to transmission rates up to the WDM's specification limits (Appendix-H).

During signal propagation several linear and nonlinear fibre impairments such as attenuation, chromatic dispersion and fibre nonlinearities affect the system. The main focus of this thesis is to study the effects of four-wave mixing (FWM) which is considered as a major limitation in a Dense Wavelength Division Multiplexing System [12].

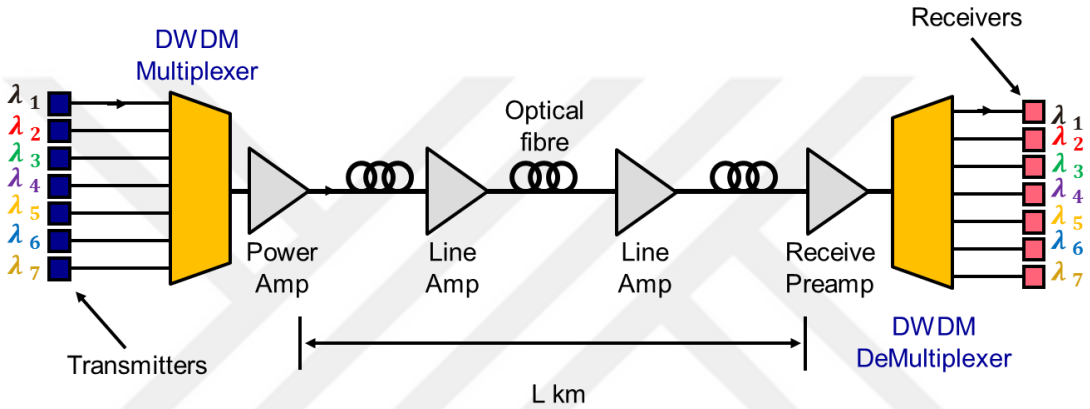

Figure 1.2: Schematic view of a DWDM System.

When low loss SMF is used (e.g, fibers with reduced OH-absorption near 1.4µm), the ultimate capacity of a WDM system can reach up to 300 nm bandwidth. The minimum channel spacing can be as small as 50 GHz or 0.4 nm for 40-Gb/s channels. Since 750 channels can fit into the 300-nm bandwidth, the resulting effective total bit rate may be as large as 30 Tb/s. Assuming that the WDM signal can be transmitted over 1000 km by using optical amplifiers with dispersion management, the effective BL product may exceed 30,000 (Tb/s).km with the usage of WDM technology [2].

1.4 Overview and Objective of the Thesis

This thesis is focused on the several degradation effects of four-wave mixing in high capacity DWDM systems. The propagation algorithm is used to calculate linear and nonlinear fiber transmission parts. The long-haul scenario is unique in the sense that it

simultaneously requires high data rates, high power levels and long distances. This is precisely the condition under which nonlinear effects are the limiting factor.

The thesis is organized as follows. The problem definition and some preliminaries on optical communication channels are given in **Chapter 1**.

Chapter 2 introduces the theoretical background of pulse propagation equation in fiber optic transmission systems. Linear and nonlinear fibre impairments effecting the transmission are presented. All of the high capacity WDM systems transmit multiple-channels on a single fiber with high spectral efficiency. The performance in these systems is limited by the inter-channel non-linearities (XPM, FWM) due to the interaction of neighbouring channels. The main focus of this work will be the effect of FWM as the most problematic nonlinear impairment of DWDM systems. The impact of intra-channel and inter-channel nonlinear effects of FWM is analyzed at 10 and 40 Gbit/s.

The signal propagation in a fiber channel can be described by the *nonlinear Schrodinger equation (NLSE)* and the solution of the NLSE can be solved numerically by using *split-step Fourier method (SSFM).*

In **Chapter 3** numerical solution of pulse propagation equation is presented. Software simulations performed in Matlab with Split Step Algorithm (SSFM). Optisystem, (or Linksim) a commercial software is used to compare and verify results. SSFM algorithm is implemented by solving the linear and nonlinear part in an iterative method numerically.

All the simulation results derived are given in **Chapter 4**. The conclusions are summarized. Several future research directions are also suggested and discussed in this chapter.

2. THEORY OF OPTICAL FIBERS

2.1 Fiber Types

An introduction to the theory of optical fibers was given in Section 1.2. In terms of the ray optics, approximation for propagation is described by the Snell's law and Total Internal Reflection. The fibers with higher fractional index change Δ are not suitable for optical communications due to the multipath dispersion (modal dispersion). For this reason, another type of fiber is developed with considerably reduced intermodal dispersion. Such an optical fiber is called as graded-index fiber (GRIN) [2].

Graded-index fibers have a core with radially decreasing refractive index from the center to the core boundary. Considering the geometrical properties and the number of guided modes, the fibers can be categorized further as multi-mode and single mode fibers.

The graded index profile is usually given as:

$$n(\rho) = \begin{cases} n_1\left[1-\Delta(\rho/\alpha)^{\alpha}\right]; & \rho < \alpha, \\ n_1\left[1-\Delta\right] = n_2; & \rho \geq \alpha \end{cases} \tag{2.1}$$

where α is the core radius. The parameter α determines the index profile. n_1 is the nominal refractive index $n_1 = n\ (r = 0)$, n_2 is the refractive index of the homogeneous cladding, ρ is the radius of the core, $\Delta = (n_1^2 - n_2^2)/2n_1^2$. A step-index profile is approached in the limit of large α. A parabolic-index fiber corresponds to $\alpha = 2$.

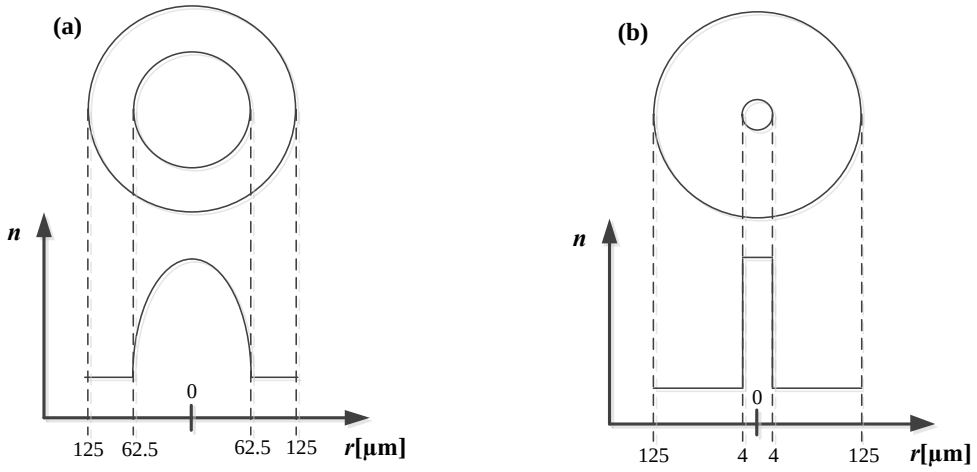

Figure 2.1: Standard geometrical parameters and index profiles for optical fibers (a) graded-index MMF, (b) step-index SMF [13].

For optical communication systems, optical fibers are assumed to be a perfect data transmission medium considering bandwidth limitations of the other mediums. Several limitations are taken into account especially in high bit rate systems, as the distance and number of amplifiers increase. These limitations can be divided into two major categories: linear and nonlinear.

The linear propagation effects of the fibers are attenuation, chromatic dispersion (CD) and polarization mode dispersion (PMD).

In particular, the nonlinear effects set strict limitations for multiwavelength WDM systems at higher bit rates and increased distances. The primary nonlinear effects are self phase modulation (SPM), cross phase modulation (CPM) and four-wave mixing (FWM).

These fiber transmission impairments are categorized in the Figure 2.2.

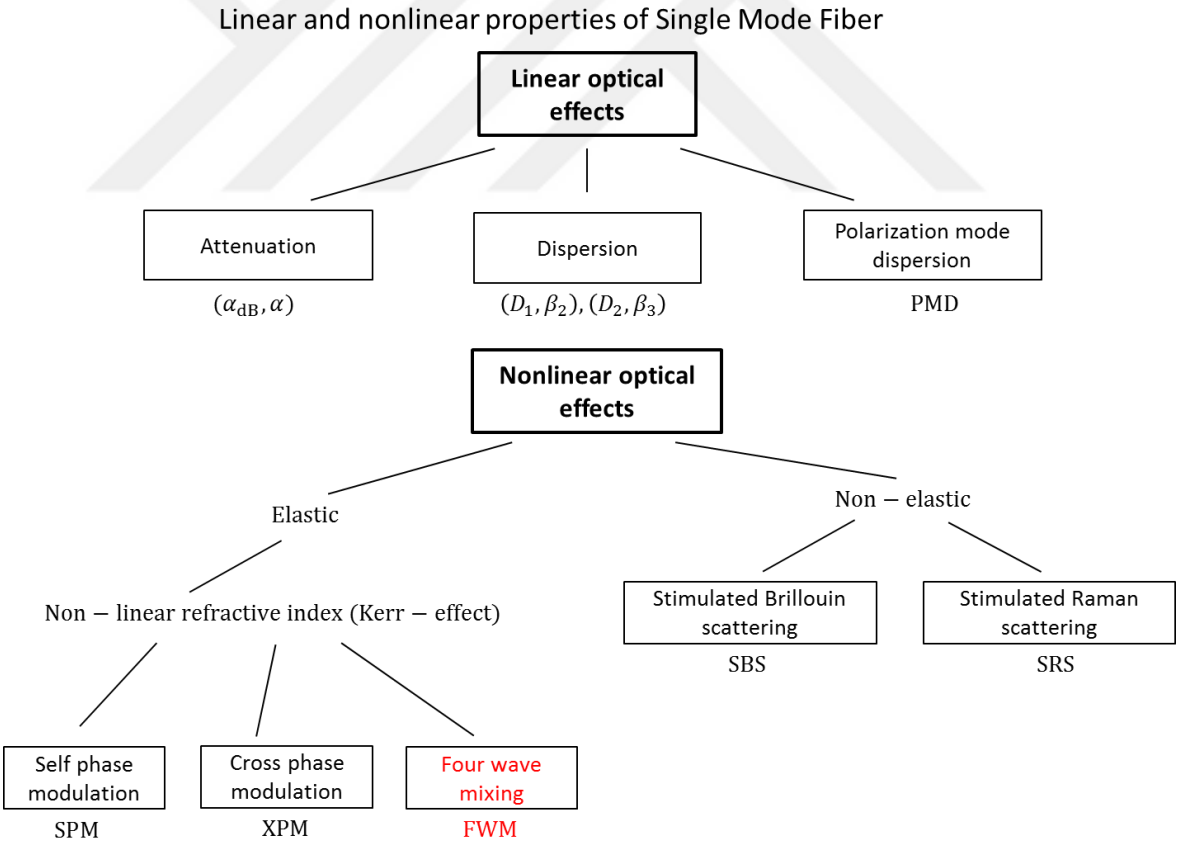

Figure 2.2: Linear and non-linear optical fiber effects.

2.2 Linear Degredation

2.2.1. Attenuation in Fibers

Average optical power P of a bit stream propagating inside an optical fiber differs and it can be shown by Beer's formula:

$$\frac{dP}{dz} = -\alpha P \tag{2.2}$$

where α is the attenuation coefficient.

Optical power loss is wavelength dependent and cumulative in an optical fiber. It increases exponentially with fiber length,

$$E_x(z,t) = E_0 e^{-\alpha z} e^{j(\omega t - \beta z)} W \tag{2.3}$$

The amount that an optical signal is attenuated in power after propagating through a passive component or fiber can be defined as optical loss and given by

$$P_{out} = P_{in} \exp(-\alpha L) \tag{2.4}$$

where P_{out} is the transmitted power, P_{in} is the initial power and L is the length of the fiber.

The value of α can be expressed in units of dB/km using the relation

$$\alpha(dB/km) = \frac{-10}{L} \log_{10}\left(\frac{p_{out}}{p_{in}}\right) \approx 4.343\alpha \tag{2.5}$$

Elastic collisions between the light wave and fiber molecules cause the scattering of light along the entire length of the fiber. This type of scattering is also known as Rayleigh scattering. Some of the light escaping from the fiber waveguide and some of the light reflecting back to the source is a direct outcome of Rayleigh scattering that causes 96% of (attenuation) signal loss in fibers. However, the other factors such as material absorption and bending loss account for the rest.

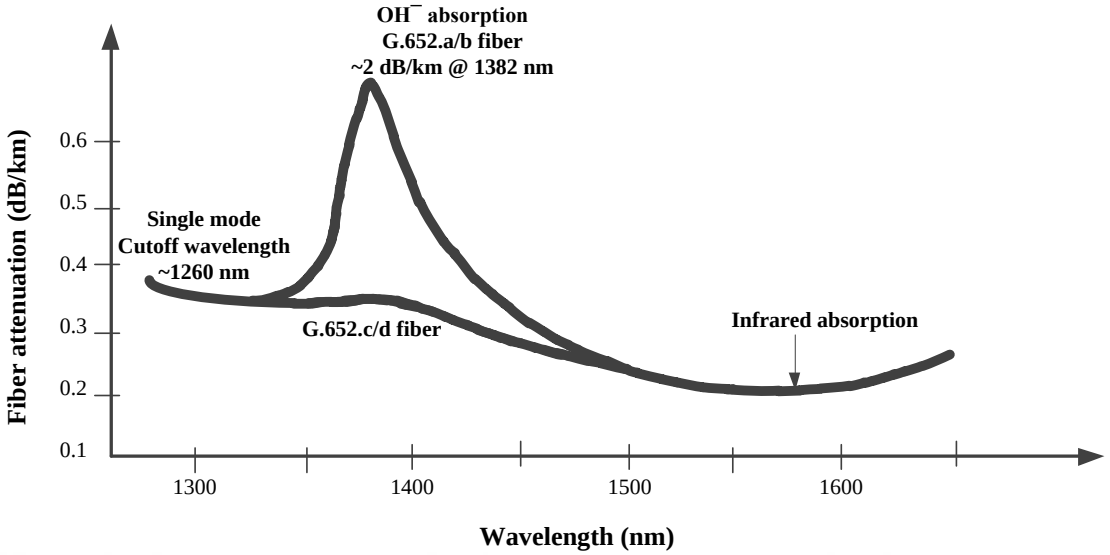

Figure 2.3: Fiber attenuation dependence on wavelength.

Absorption of light energy by fiber impurities such as water (OH−) molecules is called material absorption. The main water absorption band is centered at 1383 nm, which is considerably reduced in newer G.652.c/d fiber. Figure 2.3 shows fiber attenuation dependence on wavelength of a typical standard G.652.a/b fiber and reduced water absorption G.652.c/d fiber.

2.2.2. Chromatic Dispersion

Variation in propagation delay with respect to wavelength results in broadening of the pulses. This phenomenon is referred as Chromatic Dispersion (C.D.) which depends on fiber materials and dimensions.

Phase velocity of a propagating wave (carrier velocity) is related to propagation parameter β as defined in the equation below

$$v = \frac{\omega}{\beta} = \frac{c}{n_{eff}} \tag{2.6}$$

n_{eff} is the effective refractive (mode) index that is related to propagation constant:

$$\beta = n_{eff} k_0 \tag{2.7}$$

where k_0 is the wave number and defined as $k_0 = \omega/c = 2\pi/\lambda$.

For a single mode fiber (SMF), the major source of dispersion is the group velocity dispersion (GVD). *Group velocity* (pulse envelope velocity or information velocity) is defined as derivative of the phase velocity,

$$v_g = (d\beta/d\omega)^{-1} = 1/\beta_1 \tag{2.8}$$

where β is the propagation constant.

The wavelength dependence of the group velocity leads to pulse broadening due to the dispersion of different spectral components during propagation. Resulted *time delay* (Fig. 2.4) can be determined as

$$T = L/v_g \tag{2.9}$$

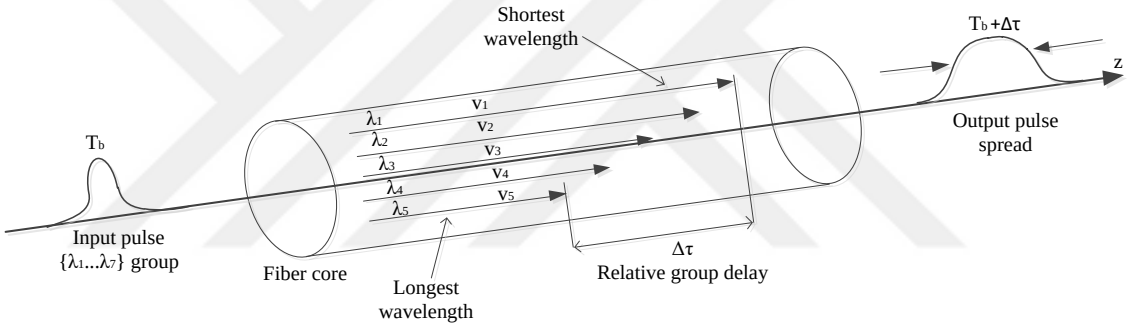

Figure 2.4: Pulse spreading due to chromatic dispersion in fiber [12].

Using Equation 2.9, the extent of broadening (ΔT) for a pulse spectral width of $\Delta\omega$ through a fiber of length L is governed by

$$\Delta T = \frac{dT}{d\omega}\Delta\omega = \frac{d}{d\omega}\left(\frac{L}{v_g}\right)\Delta\omega = L\frac{d^2\beta}{d\omega^2}\Delta\omega = L\beta_2\Delta\omega \tag{2.10}$$

β_2 is known as the *group velocity dispersion (GVD)* parameter. It's used to present pulse broadening parameter of the optical signal while propagating inside the fiber.

Dispersion coefficient can also be derived from the propagation constant with expansion of Taylor-series as

$$\beta(\omega) = n(\omega)\frac{\omega}{c_0} = \beta(\omega_0) + \left.\frac{d\beta}{d\omega}\right|_{\omega=\omega_0} \cdot \Delta\omega + \frac{1}{2}\left.\frac{d^2\beta}{d\omega^2}\right|_{\omega=\omega_0} \cdot \Delta\omega^2 + \cdots \tag{2.11}$$

where $\beta_2 = \frac{d^2\beta}{d\omega^2}$ is *group velocity dispersion (GVD)* (2.12)

Spectral width of the optical pulse is defined as

$$\Delta\omega = \left(-2\pi c/\lambda^2\right)\Delta\lambda \tag{2.13}$$

Substituting Equation 2.13 in Equation 2.10, broadening of pulse can be written as

$$\Delta T = \frac{d}{d\lambda}\left(\frac{L}{v_g}\right)\Delta\lambda = DL\Delta\lambda \tag{2.14}$$

where $D = \frac{d}{d\lambda}\left(\frac{1}{v_g}\right) = -\frac{-2\pi c}{\lambda^2}\beta_2$ (2.15)

D is called *dispersion coefficient* and can be expressed by the group velocity dispersion, β_2,

$$D = -\frac{2\pi c}{\lambda^2}\beta_2 \qquad \text{ps/(km-nm)} \tag{2.16}$$

dispersion slope is also often expressed in terms of wavelength using the dispersion slope parameter

$$S = \frac{dD}{d\lambda} = \left(\frac{2\pi c}{\lambda_0{}^2}\right)^2 \beta_3 - \frac{2}{\lambda_0} D \tag{2.17}$$

where the slope parameter *S* is normally given in ps/nm^2/km. A typical value in SMF at 1550 nm is 0.08 ps/nm^2/km.

Material dispersion and waveguide dispersion are the two subproducts of total dispersion in optical fibers.

Predominant one material (intermodal) dispersion appears in MMF because the different modes are associated with different velocities. Material dispersion occurs due to the fiber core's refractive index changing with wavelength.

It can be defined as

$$D_M = \frac{1}{c}\frac{dn_g}{d\lambda} \tag{2.18}$$

where n_g is the *group index* defined as $n_g = n_{eff} + \omega\,(dn_{eff}/d\omega)$.

At the wavelength of 1.276 μm, slope of n_g becomes zero $(dn_g/d\lambda = 0)$. This wavelength is referred to as *zero-dispersion wavelength* λ_{ZD}. For the region below λ_{ZD}, D_M is negative and above that it becomes positive. Zero dispersion wavelength of the fibers can vary depending on doping the core and cladding which results in with a refractive index variation based upon design.

The main cause of the waveguide dispersion effect is the physical structure of the fiber core cladding that causes pulses to propagate at different velocities for different wavelengths.

Waveguide dispersion depends on fiber design parameters such as core radius ρ and core-cladding index difference Δ. It can be calculated as

$$D_W = -\frac{2\pi\Delta}{\lambda^2}\left[\frac{n_g^2}{n_2\omega}\frac{Vd^2(Vb)}{dV^2} + \frac{dn_g}{d\omega}\frac{d(Vb)}{dV}\right] \tag{2.19}$$

Since the result of this equation is always negative, D_W is negative throughout the entire wavelength range [2].

If the total dispersion is considered (Figure 2.5) as the combination of material and waveguide dispersion, it reduces to

$$D = D_M + D_W \tag{2.20}$$

As the pulse propagate in fiber, signal pulse becomes wider due to chromatic disperison which leads to two major problems:

1) Trailing and leading edges of the pulse spreads into adjacent pulse bit time slots which is called as Inter Symbol Interference (ISI),
2) The spread of pulse to adjacent time slot results in decreasing in the optical power.

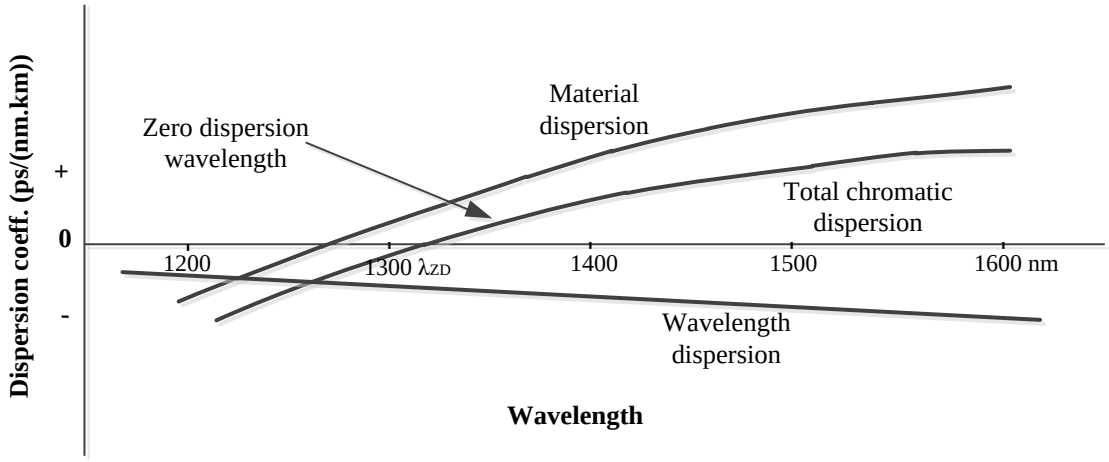

Figure 2.5: Total chromatic dispersion in SMF resulting from material and waveguide dispersion [4].

Typical values of dispersion are in the range 15–18 ps/(km-nm) near 1.55μm. In WDM communication systems, this wavelength region has remarkable interest.

Using this feature, new fibers designed such that whose zero dispersion wavelength are shifted towards the longer wavelengths.

Most commonly deployed fiber type is Standard Single Mode Fiber (SMF, ITU-T G.652) which has a non-dispersion shifted structure. Therefore it is also known as Non-Dispersion Shifted Fiber (NDSF). Zero dispersion wavelength of SMF is approximately 1310 nm. They are used for both TDM and DWDM transmission systems with the dispersion compensation requirement.

Dispersion-shifted fibers (DSF, ITU-T G.653) have its zero dispersion wavelength in 1550 nm region. This property reduces dispersion for this window whereas increasing nonlinear distortions especially FWM in deployment for DWDM links.

The other type of fiber has a low chromatic dispersion window in 1550 nm region but not zero. Those fibers which are designed to alleviate nonlinear distortions is known as Non-zero Dispersion Shifted Fiber (NZDSF, ITU-T G.655). Because of the reasons, these fibers are frequently preferred in multichannel DWDM systems.

Also fibers with the positive β_2 value ,(D negative) in the wavelength region below 1.6 μm are designated to compensate dispersion in communication links. This type of fiber is called dispersion compensating (DCF) fiber [12].

2.2.3 Polarization Mode Dispersion

Ideally, single mode fibers have perfectly cylindrical and circular core. But in industry the core of the fibers exhibit variations in the shape along with the fiber length due to mechanical and thermal stresses included during manufacturing and deployment. The change of geomety results in a difference between index of refraction and the orthogonally polarized modes.

This phenomenon is referrred to as *birefrigence* and defined as

$$B_m = \left| n_{x-eff} - n_{y-eff} \right| \tag{2.21}$$

where n_{x-eff} and n_{y-eff} are mode indices for orthogonally polarized modes.

A periodical power exchange between these two orthogonal polarization components occurs because of the birefrigence. This period is called *beat length* and can be calculated as

$$L_B = \frac{\lambda}{B_m} \tag{2.22}$$

Typically $L_B = 10$ m at 1μm.

As a result of birefrigence, initially launched linear polarization quickly reaches a state of arbitrary polarization.

These two principal states of polarization have different velocities that lead to pulse spreading along the fiber. The amount of pulse spreading in time between the two polarization pulses is referred to as *differential group delay (DGD)* and is measured in units of picoseconds (Figure 2.6).

Differential group delay is given by

$$\Delta T = \left| \frac{L}{v_{gx}} - \frac{L}{v_{gy}} \right| = L \left| \beta_{1x} - \beta_{1y} \right| = L(\Delta\beta_1) \tag{2.23}$$

When both of the polarization components of input pulse excited into a waveguide fiber, pulse becomes broader as the components disperse due to different propagation velocities (also for different frequency components) of the signal's two orthogonal polarizations.

This phenomenon is called *polarization-mode dispersion (PMD)* and turns out to be a restrictive factor for optical communication systems operating at high bit rates.

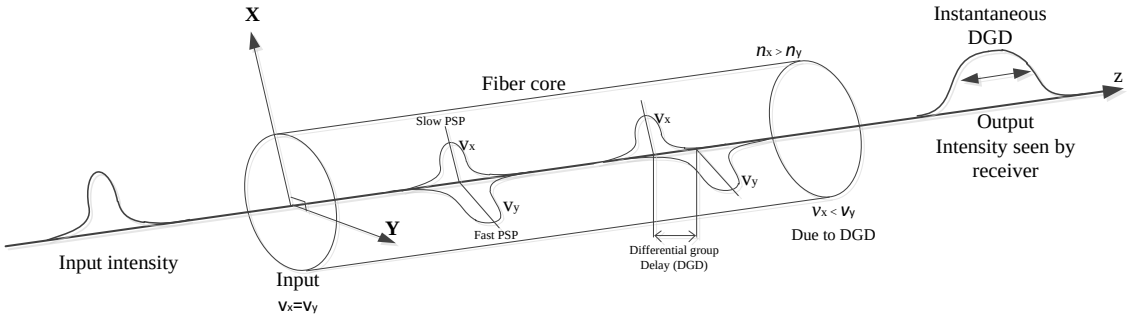

Figure 2.6: Differential group delay (PMD) effect on pulse propagation [3].

It can be calculated as;

$$D_p = \frac{\Delta T}{\sqrt{L}} \quad ps/\sqrt{km} \tag{2.24}$$

where ΔT is the differential group delay and L is the length of the fiber as a transmission distance.

PMD value is in the range of 0.1-1 ps/√km. Because of its √L dependence, PMD induced pulse broadening is relatively small as compared to GVD effects [2,12].

2.3 Nonlinear Degredations

The refractive index of the fiber is assumed to be constant at low power levels. This assumption makes silica as a linear medium. In other words the fiber material (silica) is assumed to be linear medium.

Even though silica is intrinsically not a highly nonlinear material, the waveguide geometry confines light to the small core cross section and hence power density becomes several hundreds of MW/m^2 . Thus, over long fiber spans nonlinear effects become significant in the design of WDM communication systems.

Effect of nonlinear impairments is dependent on signal strength which declines exponentially along with the propagation in the fiber. Therefore, effective fiber length is defined as the length of fiber beyond which nonlinear effects are no longer significant.

$$L_{eff} = \frac{\int_0^L P(z)dz}{P_{in}} \tag{2.25}$$

where P_{in} is the initial optical power, L is the fiber length and $P(z)$ is the power of the optical signal at length of z. $P(z)$ is related to the attenuation in the fiber:

$$P(z) = P_{in}e^{-\alpha z} \tag{2.26}$$

Thus L_{eff} can be reduced to

$$L_{eff} = \frac{1-e^{-\alpha L}}{\alpha} \tag{2.27}$$

Typically α is 0.048/km (α_{dB} = 0.21 dB/km) at 1550 nm, then L_{eff} is approximately 21 km for very long (where L>> 21 km) nonamplified fiber links.

Nonlinear effects in optical fiber mainly originate from fiber's refractive index dependence on intensity of the propagating signal which is referred to as *Kerr effect*. Variation in refractive index due to the Kerr effect is caused by two reasons.

First one is the change in refractive index due to the high signal power levels. This change in refractive index can be calculated as

$$n(\omega, E) = n_{eff}(\omega) + n_2 \frac{p}{A_{eff}} \tag{2.28}$$

where A_{eff} is the effective fiver core area, n_2 is the nonlinear index coefficient. Typical values of n_2 are 3.0 x 10^{-20} m^2/W (varies between 2.0 x 10^{-20} to 3.5 x 10^{-20} m^2/W) for silica.

Second significant reason of nonlinear Kerr effect is the change in refractive index due to the change of propagation parameter (β) by a factor called nonlinear coefficient (γ). It can be derived by

$$\beta' = \beta + \gamma P \tag{2.29}$$

where β' is the nonlinear propagation parameter.

In practice nonlinear coefficient (γ) varies between 1 to 3 (1/km.W) And it can be obtained by

$$\gamma = \frac{2\pi n_2}{\lambda A_{eff}} \tag{2.30}$$

2.3.1 Self-phase modulation

Nonlinear coefficient term (γ) produces a pahse shift which increases linearly along with the propagation distance z. This nonlinear phase modulation induces a pulse on itself which referred as Self-Phase Modulation (SPM). Assuming the constant input power, nonlinear phase shift due to SPM is given by

$$\phi^{SPM} = \int_0^L (\beta' - \beta) dz = \int_0^L \gamma P(z) dz = \gamma P_{in} L_{eff} \tag{2.31}$$

where $P(z)$ and L_{eff} are defined in Equation (2.26) and (2.27) respectively.

SPM leads to frequency chirping of optical pulses which depends on the pulse shape. In order to reduce the impact of SPM, phase shift value ϕ_{SPM} should be less than 0.1. For long fibers, this assumption can be approximated to

$$P_{in} < 0.1\ \alpha / (\gamma \cdot N_A) \tag{2.32}$$

In practice, if γ=2 (1/W.km), N_A=10, α=0.2 dB/km, the input peak power is limited to 2.2 mW.

2.3.1 Cross-phase modulation

The nonlinear behaviour of the refractive index due to the optical intensity of other channels creates phase shift (i.e. frequency modulation) for a specific channel. This phenomena is known as *cross-phase modulation (CPM or XPM)* which occurs especially in multichannel transmission systems such as DWDM.

Phase shift of the j-th channel can be written as

$$\phi_j^{XPM} = \gamma L_{eff} (P_j + 2 \sum_{m \neq j} P_m) \tag{2.33}$$

Assuming equal channel powers worst case of the phase shift occurs when pulses completely overlap one another. In this case phase shift can be estimated as

$$\phi_j^{XPM} = (\gamma/\alpha)\ (2M-1)P_j \tag{2.34}$$

Pulses at different wavelengths travel at different group velocities in the presence of dispersion and cause walk-off between pulses. This process diminishes the distortions induced by XPM. Therefore, the effect of XPM is inversely proportional to dispersion discrepancies among channels in WDM systems [2,12].

2.4 Four-Wave Mixing

2.4.1 Introduction

In WDM transmission, when three optical signals of different center wavelengths are propagating through an optical fiber, beating (mixing) of the signals leads to generation of interfering signals at new wavelengths. This process is called as Four-Wave Mixing (FWM). This newly produced signal is called FWM component which can cause signal crosstalk if the frequency falls within the band of an existing WDM channel. FWM originates from the dependence of the fiber's refractive index on the intensity of optical signal that produces a nonlinear medium due to the third order nonlinear susceptibility. If the number of channels are increased, number of FWM light is also increased. It can be expressed as

$$\omega_4 = \omega_1 \pm \omega_2 \pm \omega_3 \tag{2.35}$$

But only frequency combinations of $\omega_4 = \omega_1 \pm \omega_2 \pm \omega_3$ are generate significantly high power components in WDM systems provided that the channel spacing and dispersion are small enough to meet the phase matching condition.

FWM process is also different from SPM and XPM because of energy transfer between channels. Such a power transfer not only results in the power loss for the channel but also induces interchannel crosstalk that degrades the system performance seriously.

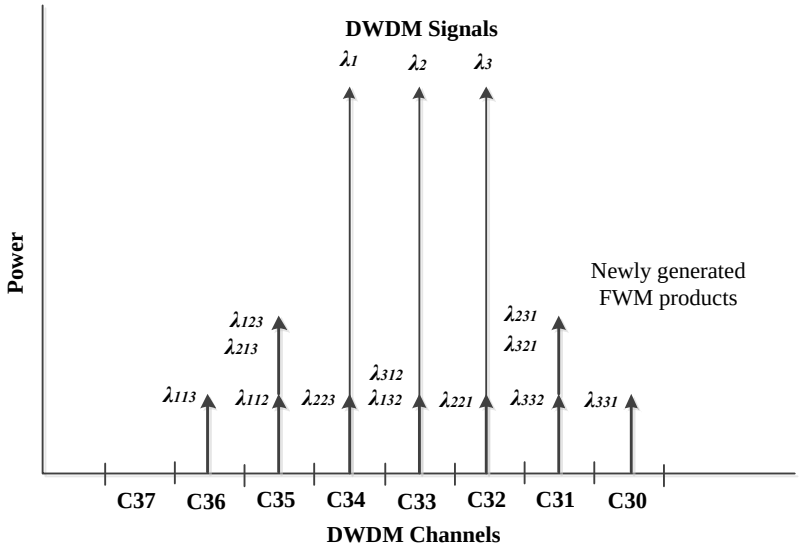

Figure 2.7: FWM products of three equally spaced DWDM signals [12].

In Table 2.1 three equally spaced DWDM channels (λ_1=1550.12, λ_2=1550.92, λ_3=1551.72 nm) and FWM components is presented. Generated FWM terms are given in Table 2.1.

Table 2.1: FWM products of three equally spaced DWDM channels.

Generated interfering wavelength	**Channel Assignmet (ITU-T)**
λ_{113}=1548.52 nm	channel 36
λ_{123}=1549.32 nm , λ_{213}=1549.32 nm	channel 35
λ_{112}=1549.32 nm	channel 35
λ_{223}^{*}=1550.12 nm	channel 34
λ_{312}^{*}=1550.92 nm, λ_{132}=1550.92 nm	channel 33
λ_{221}^{*}=1551.72 nm	channel 32
λ_{332}=1552.52 nm	channel 31
λ_{321}=1552.52 nm, λ_{231}=1552.52 nm	channel 31
λ_{331}=1553.32 nm	channel 30

The generated components with center wavelengths λ_{223}=1550.12, λ_{312}=1550.92, λ_{221}=1551.72 fall directly into the original DWDM signal channels therefore causing interference. The other generated components fall into adjacent and nearby DWDM channels interfering with those channels (Figure 2.7) [2,12].

Total number of generated FWM components is calculated by

$$\frac{N^2(N-1)}{2} \tag{2.36}$$

where N is the number of DWDM channels.

Assuming channels are equally spaced and number of channels are even, the number of these FWM components on the m-th signal channel is expressed as

$$N_{FWM} = \frac{N^2}{4} + \frac{Nm}{2} - \frac{m^2}{2} - N + \frac{m}{2} \tag{2.37}$$

Therefore, the total number of the FWM components that fall on the signal channels can be calculated as:

$$\begin{aligned} N_{FWM,total} &= \sum_{m=1}^{N} N_{FWM,m} \\ &= N \cdot \frac{N^2}{4} + \frac{N(1+2+\cdots+N)}{2} - \frac{1^2+2^2+\cdots+N^2}{2} - N \cdot N + \frac{1+2+\cdots+N}{2} \\ &= \frac{N^3}{4} + \frac{N+1}{2} \cdot \frac{N^2+N}{2} - \frac{1}{12} N(N+1)(2N+1) - N^2 \\ &= \frac{1}{3}N^3 - \frac{3}{4}N^2 + \frac{1}{6}N \end{aligned} \tag{2.38}$$

As number of channels increases, generated FWM products increases rapidly.

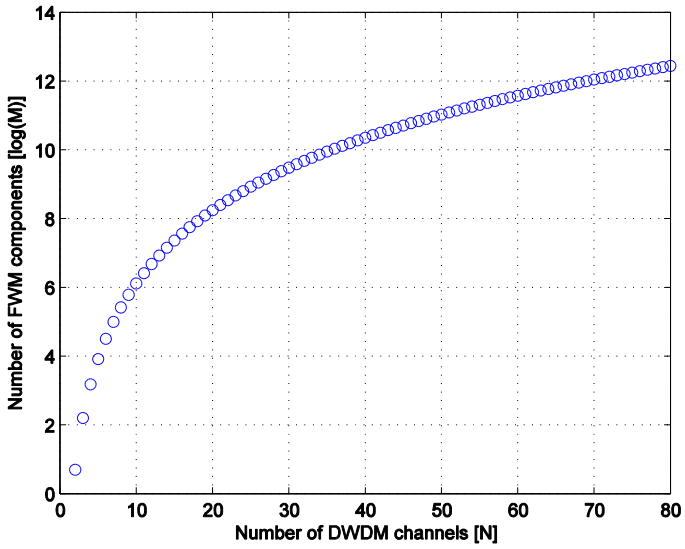

Figure 2.8: Number of FWM components.

2.4.2 FWM Efficiency

FWM leads to crosstalk and this resulting with the generation of new wave at frequency can be defined by

$$\omega_{FWM} = \omega_i + \omega_j - \omega_k$$

Types of mixing are divided to two categories as degenerate and non-degenerate. Degenerate involves FWM components that do not appear on the original DWDM signal channels ($f_i = f_j \neq f_k$). Nondegenerate involves FWM components that can appear on the same original DWDM signal channels ($f_i \neq f_j \neq f_k$).

Assuming all signals have the same polarization along the propagation in the fiber and no amplifiers are used, the power of FWM component can be calculated as

$$P_{ijk} = \frac{1}{9}\eta d^2 \gamma^2 P_i P_j P_k (L_{eff})^2 e^{-\alpha L} \tag{2.39}$$

where η is the *efficiency* and d is the *degeneracy factor* which defined as

$$d_{ijk} = \begin{cases} 3, & i = j \\ 6, & i \neq j \end{cases}$$

FWM efficiency can be obtained as

$$\eta = \frac{\alpha^2}{\alpha^2 + \Delta\beta^2}\left[1 + \frac{4e^{-\alpha L}\sin^2(\Delta\beta L/2)}{(1-e^{-\alpha L})^2}\right] \tag{2.40}$$

where $\Delta\beta$ is the phase mismatch.

Assuming same channel spacing, phase mismatch parameter can be given by (Appendix-E).

$$\Delta\beta = \frac{2\pi\lambda_k^2}{c}\Delta f_{ik}\Delta f_{jk}\left[\mathrm{CD}_c + \frac{\lambda_k^2}{2c}(\Delta f_{ik} + \Delta f_{jk})S_{\mathrm{fc}}\right] \tag{2.41}$$

Assuming the same channel spacing, depending on the distance of center wavelength of the DWDM system to the zero-dispersion wavelength phase mismatch parameter , $\Delta\beta$,can be reduced to

$$\Delta\beta = \begin{cases} \frac{2\pi\lambda_0^4}{c^2}\Delta f^2(f_i - f_0)S & \lambda_m \text{ is near } \lambda_0 \\ \frac{2\pi\lambda_m^2 D_c}{c}\Delta f^2 & \lambda_m \text{ is far from } \lambda_0 \end{cases} \tag{2.42}$$

The FWM efficiency is shown in Figure 2.9 as a function of channel spacing. Fiber dispersion coefficient for a 100 km fiber span with attenuation is also taken 0.21 dB/km at 1550 nm. As the fiber's dispersion coefficient or channel spacing increases, the FWM efficiency decreases, thereby reducing the power of FWM component. As the CD increases, the FWM becomes negligible especially for the broader channel spacing.

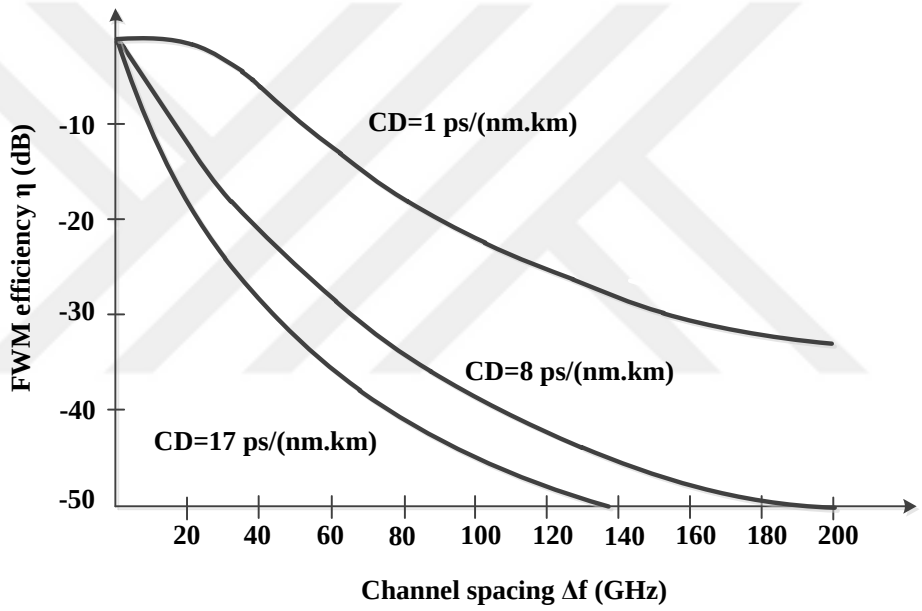

Figure 2.9: FWM efficiency for different channel spacing with respect to different values of chromatic dispersion [12].

For the long-distance transmission in WDM system, if the standard SMF is employed at 1550nm window, a cumulative CD will degrade the system performance. Due to the GVD, different channels travel at different speeds thereby lowering FWM efficiency.

When the perfect phase matching occurs the efficiency takes its the highest value, e.g. in a fibre without chromatic dispersion. Higher fibre dispersion and larger channel spacing decrease the phase matching [13].

2.4.3 Reducing FWM Effect

Numerous techniques have been proposed to reduce the effect of FWM-induced degradation on WDM systems. Generally these techniques focused on the minimizing of FWM terms that intersect with WDM channels. These techniques consist of

1- Designing WDM systems with unequal channel spacing: In order to prevent overlapping of generated FWM components on the WDM channels, uneven channel spacing can be designed.
2- Designing WDM systems with wide channel spacing: As the spacing between DWDM channels are increased, phase-matching is decreased with a result of reduced FWM efficiency.
3- Reducing transmitter signal power and amplifier spacing can help diminishing the FWM effect.
4- Deploying a fiber with larger cross sectional area (i.e. ITU-T G.655). Larger effective area reduces the optical intensity and consequently effects of FWM.

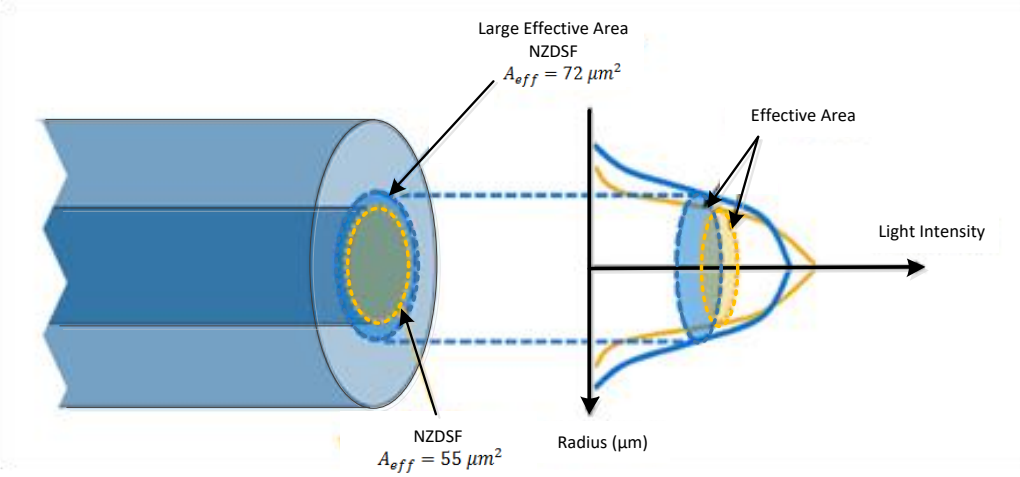

Figure 2.10: Cross sectional area of a G.655 fiber.

5- Using polarization-multiplexed DWDM channels can reduce FWM component power and cross talk.

If deployed optical fiber is not a ITU G.655 type fiber, another practical and applicable solution is to plan a dispersion-management map such that GVD is high locally all along the fiber even though its average value is quite low. Such a dispersion map can be realized with the combinations of fibers with normal and anomalous GVD. Consequently, locally high GVD leads to reduce of phase mismatch and hence resulting in a reduced FWM crosstalk [13].

3. PULSE PROPAGATION IN WDM OPTICAL FIBER CHANNEL

3.1 Wave Propagation Equation

Maxwell equations govern the propagation of optical fields.

$$\nabla \times \mathbf{H} = \mathbf{J} + \frac{\partial \mathbf{D}}{\partial t}, \tag{3.1}$$

$$\nabla \times \mathbf{E} = -\frac{\partial \mathbf{B}}{\partial t}, \tag{3.2}$$

$$\nabla . \mathbf{D} = \rho_f , \tag{3.3}$$

$$\nabla . \mathbf{B} = 0, \tag{3.4}$$

where **E** and **H** are electric and magnetic field vectors, **D** and **B** are corresponding electric and magnetic flux densities, **J** and ρ_f are current density vector and the charge density, respectively.

Since following assumptions can be made:

- There are no free charges $\rho_f = 0$.
- Conductivity is very close to zero ($\sigma \approx 0,$ assuming a lossless medium $\mathbf{J} = \sigma . \mathbf{E}$, $\mathbf{J} = 0$).
- Silica is a nonmagnetic material.

The flux densities **D** and **B** are related to the electric and magnetic fields **E** and **P** propagating inside the medium as

$$\mathbf{D} = \varepsilon_0 \mathbf{E} + \mathbf{P} \tag{3.5}$$

$$\mathbf{B} = \mu_0 \mathbf{H} \tag{3.6}$$

where $\varepsilon_0 = 8.885 \times 10^{-12}$ As/Vm is the vacuum permittivity, $\mu_0 = 1.2566 \times 10^{-6}$ Vs/Am is the vacuum permeability, and **P** is the induced electric polarization.

Equations 3.1 to 3.4 take the following form for propagation in optical fibers

$$\nabla \times \mathbf{E} = -\frac{\partial B}{\partial t} \tag{3.7}$$

$$\nabla \times \mathbf{H} = \frac{\partial D}{\partial t} \tag{3.8}$$

$$\nabla . \mathbf{D} = 0 \tag{3.9}$$

$$\nabla . \mathbf{B} = 0 \tag{3.10}$$

Putting equations (3.1), (3.2), (3.5) and (3.6) together and taking the curl leads to

$$\nabla \times \nabla \times \mathbf{E} = -\frac{\partial}{\partial t}(\nabla \times \mathbf{B}), \tag{3.11}$$

$$\nabla \times \nabla \times \mathbf{E} = -\frac{\partial}{\partial t}\left(\mu_0 \left(\frac{\partial}{\partial t}(\varepsilon_0 \mathbf{E} + \mathbf{P})\right)\right), \tag{3.12}$$

$$\nabla \times \nabla \times \mathbf{E} = -\mu_0 \varepsilon_0 \frac{\partial^2 \mathbf{E}}{\partial t^2} - \mu_0 \frac{\partial^2 \mathbf{P}}{\partial t^2} \tag{3.13}$$

where

$$\mu_0 \varepsilon_0 = \frac{1}{c^2}, \tag{3.14}$$

Equation (3.13) yields

$$\nabla \times \nabla \times \mathbf{E} = -\frac{1}{c^2}\frac{\partial^2 \mathbf{E}}{\partial t^2} - \mu_0 \frac{\partial^2 \mathbf{P}}{\partial t^2} \tag{3.15}$$

In order to solve Equation (3.15), a relation between induced polarization vector **P** and electric field vector **E** is needed.

Induced polarization consists of two parts: linear ($\mathbf{P_L}$) and nonlinear ($\mathbf{P_{NL}}$) .

$$\mathbf{P}(\mathbf{r},t) = \mathbf{P}_L(\mathbf{r},t) + \mathbf{P}_{NL}(\mathbf{r},t). \tag{3.16}$$

$$\mathbf{P}_L(\mathbf{r},t) = \varepsilon_0 \int_{-\infty}^{+\infty} \chi^{(1)}(t-t').\mathbf{E}(\mathbf{r},t')dt', \tag{3.17}$$

$$\mathbf{P}_{NL}(\mathbf{r},t) = \varepsilon_0 \int_{-\infty}^{+\infty}\int_{-\infty}^{+\infty}\int_{-\infty}^{+\infty} \chi^{(3)}(t-t_1,t-t_2,t-t_3) \vdots \mathbf{E}(\mathbf{r},t_1)\mathbf{E}(\mathbf{r},t_2)\mathbf{E}(\mathbf{r},t_3)dt_1 dt_2 dt_3. \tag{3.18}$$

Since optical fibers (silica) are isotropic and symmetric compounds, second order nonlinear susceptibility is ignored in calculations.

Nonlinear part of polarization is a result of third order susceptibility $\chi^{(3)}$ as explained in (Appendix-A)

Due to the weakness of nonlinear effecs in silica fibers; it's considered as $\mathbf{P_{NL}}$ has a small perturbation on total polarization. It will be assumed as $\mathbf{P_{NL}} = 0$ and only linear part of the polarization will be taken into account as a first step.

Using the Equation (3.17) in Equation (3.15), yields

$$\nabla\times\nabla\times\mathbf{E}=-\frac{1}{c^2}\frac{\partial^2\mathbf{E}}{\partial t^2}-\mu_0\frac{\partial^2}{\partial t^2}\left(\varepsilon_0\int_{-\infty}^{+\infty}\chi^{(1)}(t-t').\mathbf{E}(\mathbf{r},t')dt'\right). \tag{3.19}$$

Taking Fourier transform and simplifying both sides of Equation (3.19) leads to

$$\begin{aligned}\nabla\times\nabla\times\tilde{\mathbf{E}}(\mathbf{r},\omega)&=\frac{\omega^2}{c^2}\tilde{\mathbf{E}}(\mathbf{r},\omega)+\frac{\omega^2}{c^2}\chi^{(1)}(\omega)\tilde{\mathbf{E}}(\mathbf{r},\omega)\\&=\frac{\omega^2}{c^2}(1+\chi^{(1)})\tilde{\mathbf{E}}(\mathbf{r},\omega),\end{aligned} \tag{3.20}$$

$$\nabla\times\nabla\times\tilde{\mathbf{E}}(\mathbf{r},\omega)-\varepsilon(\omega)\frac{\omega^2}{c^2}\tilde{\mathbf{E}}(\mathbf{r},\omega)=0, \tag{3.21}$$

where $\tilde{\mathbf{E}}$ (**r**,ω) is the Fourier transform of **E**(**r**,t) and it's given by

$$\tilde{\mathbf{E}}(\mathbf{r},\omega)=\int_{-\infty}^{+\infty}\mathbf{E}(\mathbf{r},t)\exp(i\omega t)dt \tag{3.22}$$

here *ε(ω)* is frequency dependent dielectric constant and related to the susceptibility as

$$\varepsilon(\omega)=\left(1+\chi^{(1)}(\omega)\right), \tag{3.23}$$

where $\tilde{\chi}^{(1)}(\omega)$ is Fourier transform of $\tilde{\chi}^{(1)}(t)$. Since $\tilde{\chi}^{(1)}(\omega)$ is generally complex, therefore $\varepsilon(\omega)$ is also complex. The real and imaginary parts of $\varepsilon(\omega)$ are related to refractive index $n(\omega)$ and absorption coefficient $\alpha(\omega)$ by

$$\varepsilon(\omega)=\left(n(\omega)+\frac{i\alpha(\omega)c}{2\omega}\right)^2. \tag{3.24}$$

Using the Equation (3.23) and (3.24) following relation can be obtained

$$1+\tilde{\chi}^{(1)}(\omega)=n^2-\left(\frac{\alpha c}{2\omega}\right)^2+n\frac{i\alpha c}{\omega} \tag{3.25}$$

Real and imaginary components in Equation (3.25) can be simplified as

$$\alpha(\omega)=\frac{\omega}{nc}\mathrm{Im}\left[\tilde{\chi}^{(1)}(\omega)\right] \tag{3.26}$$

$$n^2=1+\mathrm{Re}\left[\tilde{\chi}^{(1)}(\omega)\right], \tag{3.27}$$

$$n=\left(1+\mathrm{Re}\left(\tilde{\chi}^{(1)}(\omega)\right)\right)^{\frac{1}{2}} \tag{3.28}$$

Using the binomial expansion, Equation (3.28) reduces to

$$n(\omega) = 1 + \frac{1}{2}\mathrm{Re}\left[\tilde{\chi}^{(1)}(\omega)\right]. \tag{3.29}$$

Since $n(\omega)$ often behaves independently of spatial coordinates in both the core and cladding of step index fibers, the following identity can be used

$$\nabla \times \nabla \times \mathbf{E} = \nabla(\nabla.\mathbf{E}) - \nabla^2\mathbf{E}. \tag{3.30}$$

Using $\rho_f = 0$, it can be easily deduced that $\nabla.\mathbf{E} = 0$. Thus,

$$\nabla \times \nabla \times \mathbf{E} = -\nabla^2\mathbf{E}. \tag{3.31}$$

Another simplification can be made by considering the fact that, the imaginary part of $\varepsilon(\omega)$ is small, in comparison to the real part because of low loss of optical fiber in the wavelength region of interest. Thus, in Equation (3.24), $\varepsilon(\omega)$ can be replaced by $n^2(\omega)$.

With this simplification wave equation in equation (3.21) is simplified to

$$\nabla^2\ \tilde{\mathbf{E}}(\mathbf{r},\omega) + n^2(\omega)\frac{\omega^2}{c^2}\tilde{\mathbf{E}}(\mathbf{r},\omega) = 0 \tag{3.32}$$

3.2 Fiber Modes

Even though the nonlinear effects in optical fibers have a key role, they can be omitted in the discussion of fiber modes.

An ***optical mode*** means to a specific solution of the wave equation that satisfies the appropriate boundary conditions. Also an optical mode's spatial distribution does not change with propagation. Signal transmission in fiber-optic communication systems occurs through the guided modes only. In the remainig part of chapter, guided modes of a step-index fiber will be explained [2].

Depending on the cylindrical symmetry of the optical fibers, Equation (3.32) can be represented in cylindrical coordinates: ρ, φ and z. Applying the Laplacian operator ∇^2 in cylindrical form, given as

$$\frac{\partial^2\tilde{\mathbf{E}}}{\partial\rho^2} + \frac{1}{\rho}\frac{\partial\tilde{\mathbf{E}}}{\partial\rho} + \frac{1}{\rho^2}\frac{\partial^2\tilde{\mathbf{E}}}{\partial\phi^2} + \frac{\partial^2\tilde{\mathbf{E}}}{\partial z^2} + n^2k_0^2\tilde{\mathbf{E}} = 0 \tag{3.33}$$

where

$$\nabla^2 = \frac{\partial^2}{\partial\rho^2} + \frac{1}{\rho}\frac{\partial}{\partial\rho} + \frac{1}{\rho^2}\frac{\partial^2}{\partial\phi^2} + \frac{\partial^2}{\partial z^2}, \tag{3.34}$$

$$k_0 = \frac{\omega}{c} = \frac{2\pi}{\lambda}, \tag{3.35}$$

where n is the refractive index.

For a fiber having core radius a, $n = n_1$ for $\rho \le a$ (means inside the core) and $n = n_c$ for $\rho > a$ (means outside the core), $\tilde{\mathbf{E}}(\mathbf{r},\omega)$ is the Fourier transform of $\mathbf{E}(\mathbf{r},t)$ defined as

$$\mathbf{E}(\mathbf{r},t) = \frac{1}{2\pi}\int_{-\infty}^{+\infty} \tilde{\mathbf{E}}(\mathbf{r},\omega)\exp(-i\omega t)d\omega. \tag{3.36}$$

The wave equation for $\tilde{E}_z$ can be solved using the method of variables separation which takes the following general form as

$$\tilde{E}_z(\mathbf{r},\omega) = A(\omega)F(\rho)\exp(\pm im\phi)\exp(i\beta z), \tag{3.37}$$

where $A(\omega)$ is a normalization constant, $F(\rho)$ is the radial component of $\tilde{E}_z$, m is an integer, and β is propagation constant.

$$\frac{d^2F}{d\rho^2} + \frac{1}{\rho}\frac{dF}{d\rho} + \left(n^2k_0^2 - \beta^2 - \frac{m^2}{\rho^2}\right)F = 0. \tag{3.38}$$

To analyze the fiber **core region** ($\rho \le a$) it can be deduced that

$$\frac{d^2F}{d\rho^2} + \frac{1}{\rho}\frac{dF}{d\rho} + \left(n^2k_0^2 - \beta^2 - \frac{m^2}{\rho^2}\right)F = 0. \tag{3.39}$$

where

$$\kappa^2 = n_1^2k_0^2 - \beta^2 \tag{3.40}$$

This is a well-known Bessel differential equation, whose general solution is given by

$$F(\rho) = C_1J_m(\kappa\rho) + C_2N_m(\kappa\rho) \tag{3.41}$$

$$F(\rho) = J_m(\kappa\rho) \text{ for } \rho \le a. \tag{3.42}$$

For analysis of wave propagation in the **cladding region** (i.e. for $\rho > a$), substitute the following relation in Equation (3.38)

$$\gamma^2 = \beta^2 - n_2^2k_0^2 \tag{3.43}$$

Solution of Helmholtz equation can be considered as follows:

$$\frac{d^2F}{d\rho^2}+\frac{1}{\rho}\frac{dF}{d\rho}+\left(\gamma^2+\frac{m^2}{\rho^2}\right)F=0. \tag{3.44}$$

For cladding region, the solution $F(\rho)$ is given by

$$F(\rho)=K_m(\gamma\rho) \text{ for } \rho \geq a. \tag{3.45}$$

where K_m represents a modified Bessel function such that the solution $F(\rho)$ decays exponentially for larger values of ρ

The equations given can be limited to SMF using the following procedure.

$\kappa^2 = n_1^2 k_0^2 - \beta^2$ and $\gamma^2 = \beta^2 - n_2^2 k_0^2$ can be combined as follows;

$$\kappa^2+\gamma^2=(n_1^2-n_2^2)k_0^2. \tag{3.46}$$

Cut-off frequency is an important parameter for each mode. This frequency can be determined by setting the condition $\gamma = 0$ ($n_2=\beta/k_0$) in Equation (3.46) which is called as *cutoff condition* leads to

$$\kappa_c = k_0\sqrt{(n_1^2-n_2^2)} \tag{3.47}$$

Using the relation (3.47), a *normalized frequency V* can be defined as

$$V = a.\kappa_c = a.k_0.\sqrt{(n_1^2-n_2^2)} \tag{3.48}$$

To achieve the condition of single mode fiber, V must be smaller than V_c where $V_c \approx 2.405$.

3.2.1 Single Mode Condition

The *single-mode condition* is determined by the value of V at which the TE 01 and TM01 modes reach cutoff. A fiber designed such that $V < 2.405$ supports only the fundamental HE_{11} mode namely the single-mode condition.

For the operating wavelength range 1.3–1.6 μm, the fiber is generally designed to become single mode for $\lambda>1.2$ μm. By taking $\lambda=1.2\mu m$, $n_1=1.45$, and $\Delta=5\times10^{-3}$, Equation (3.44) shows that $V<2.405$ for a core radius $a<3.2\mu m$. The required core radius can be increased

to about 4 μm by decreasing Δ to 3×10^{-3}. Indeed, most telecommunication fibers are designed with a ≈ 4μm.

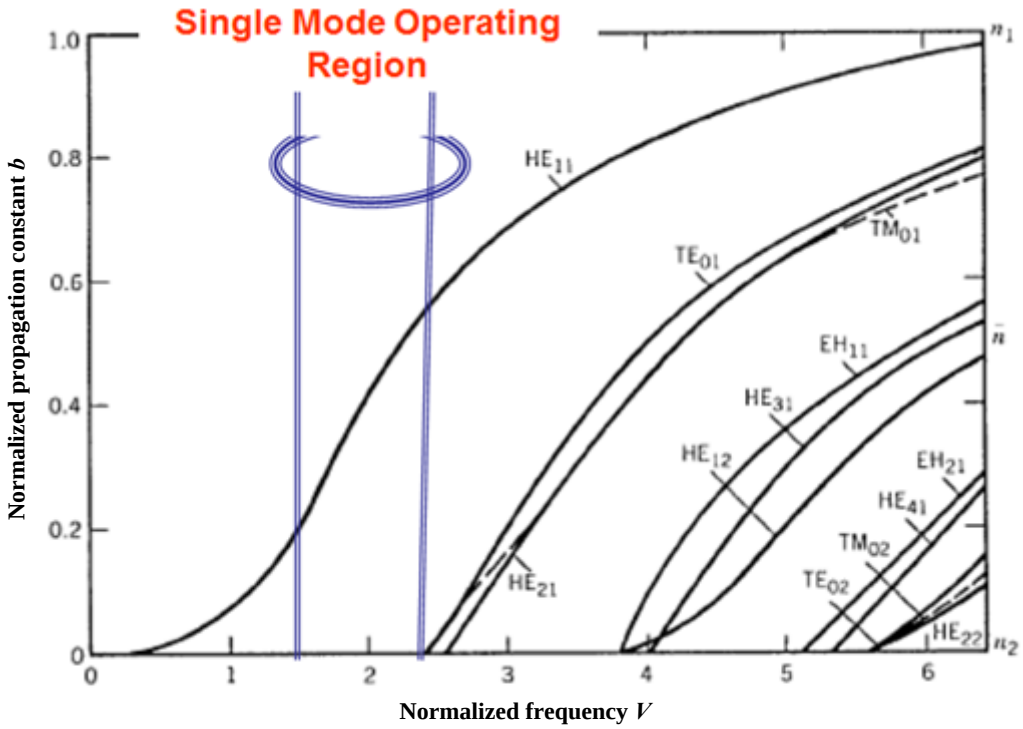

Figure 3.1: Normalized propagation constant *b* as a function of normalized frequency *V* for a few low-order fiber modes [2].

3.3 Pulse Propagation Equation

Optical fiber can be considered isotropic and ρ = 0, therefore $\nabla\mathbf{E}$ vanishes $(\nabla\mathbf{D} = \varepsilon_0\nabla\mathbf{E} = 0)$.

Recalling wave equation in (3.15) and using relation $\nabla\times\nabla\times\mathbf{E} = \nabla(\nabla\mathbf{E}) - \nabla^2\mathbf{E} = -\nabla^2\mathbf{E}$,

Wave equation takes the following form

$$\nabla^2\mathbf{E} - \frac{1}{c^2}\frac{\partial^2\mathbf{E}}{\partial t^2} = \mu_0\frac{\partial^2\mathbf{P}}{\partial t^2} \tag{3.45}$$

Using the linear and nonlinear representation of polarization, wave equation is given by

$$\nabla^2\mathbf{E}-\frac{1}{c^2}\frac{\partial^2\mathbf{E}}{\partial t^2}=\mu_0\frac{\partial^2\mathbf{P}_L}{\partial t^2}+\mu_0\frac{\partial^2\mathbf{P}_{NL}}{\partial t^2}$$
$$\mathbf{P}_L=\varepsilon_0\ \chi^{(1)}\mathbf{E}, \tag{3.46}$$
$$\mathbf{P}_{NL}=\varepsilon_0\ \chi^{(3)}\mathbf{EEE}$$

and $\boldsymbol{P}_{\mathbf{L}}$ denotes the linear part while $\boldsymbol{P}_{\mathbf{NL}}$ the nonlinear part of the induced polarization vector.

It will be assumed that the wave will maintain its polarization along the fiber length.

The optical field is considered to be quasi-monochromatic ($\Delta\omega/\omega_0 \ll 1$ where ω_0 is the center frequency and $\Delta\omega$ is the spectral width).

P_{NL} is treated as a small perturbation compared to P_L (nonlinear effects are weak in silica fibers).

$$\mathbf{P}(\mathbf{r},t)=\varepsilon_0\int_{-\infty}^{+\infty}\chi^{(1)}(t-\tau)\mathbf{E}(\mathbf{r},\tau)\mathrm{d}\tau+$$
$$\varepsilon_0\int\int_{-\infty}^{+\infty}\chi^{(2)}(t-\tau,t-\theta)\mathbf{E}(\mathbf{r},\tau)\mathbf{E}(\mathbf{r},\theta)\mathrm{d}\tau\mathrm{d}\theta+$$
$$\varepsilon_0\int\int\int_{-\infty}^{+\infty}\chi^{(3)}(t-\tau,t-\theta,t-\eta)\mathbf{E}(\mathbf{r},\tau)\mathbf{E}(\mathbf{r},\theta)\mathbf{E}(\mathbf{r},\eta)\mathrm{d}\tau\mathrm{d}\theta\mathrm{d}\eta+\ldots$$

$$\mathbf{P}(\mathbf{r},t)\approx\varepsilon_0\ \left[\chi^{(1)}\mathbf{E}(\mathbf{r},t)+\chi^{(2)}\mathbf{E}(\mathbf{r},t)\mathbf{E}(\mathbf{r},t)+\chi^{(3)}\mathbf{E}(\mathbf{r},t)\mathbf{E}(\mathbf{r},t)\mathbf{E}(\mathbf{r},t)\right] \tag{3.47}$$

Rapidly varying part of the electric field is seperated according to slowly varying envelope approximation in the following form

$$\mathbf{E}(\mathbf{r},t)=\frac{1}{2}\hat{x}\left[E(\mathbf{r},t)\exp(-i\omega_0 t)+E^*(\mathbf{r},t)\exp(i\omega_0 t)\right], \tag{3.48}$$

where $\hat{x}$ is the polarization unit vector of the light assumed to be linearly polarized along the *x* axis, **E**(**r**, t) is a slowly-varying function of time (relative to the optical period) and $\mathbf{E}^*$ means the complex conjugate of **E**.

In the same manner, the material polarization components $\mathbf{P}_L$ and $\mathbf{P}_{NL}$ are expressed as

$$\mathbf{P}_L(\mathbf{r},t)=\frac{1}{2}\hat{x}\left[P_L(\mathbf{r},t)\exp(-i\omega_0 t)+P_L{}^*(\mathbf{r},t)\exp(i\omega_0 t)\right],$$
$$\mathbf{P}_{NL}(\mathbf{r},t)=\frac{1}{2}\hat{x}\left[P_{NL}(\mathbf{r},t)\exp(-i\omega_0 t)+P_{NL}{}^*(\mathbf{r},t)\exp(i\omega_0 t)\right]. \tag{3.49}$$

Considering only linear polarization if we substitute Equation (3.48) into Equation (3.49), it takes the form as

$$\mathbf{P}_L(\mathbf{r},t) = \varepsilon_0 \int_{-\infty}^{+\infty} \chi_{xx}^{(1)}(t-t')E(\mathbf{r},t')\exp\left[i\omega_0(t-t')\right]dt'. \tag{3.50}$$

Fourier transform of this equation will be as follows

$$P_L(\mathbf{r},\omega-\omega_0) = \varepsilon_0 \int_{-\infty}^{+\infty}\int_{-\infty}^{+\infty} \chi^{(1)}{}_{xx}(t-t')E(\mathbf{r},t')\exp\left[i\omega_0(t-t')\right]dt'\exp\left[i(\omega-\omega_0)t\right]dt,$$

$$P_L(\mathbf{r},\omega-\omega_0) = \varepsilon_0 \int_{-\infty}^{+\infty}\int_{-\infty}^{+\infty} \chi^{(1)}{}_{xx}(t-t')E(\mathbf{r},t')\exp(-i\omega_0 t' + i\omega t)dt'dt, \tag{3.51}$$

$$P_L(\mathbf{r},\omega-\omega_0) = \varepsilon_0\ \chi^{(1)}{}_{xx}(\omega)E(\mathbf{r},\omega-\omega_0).$$

Taking the inverse Fourier transform, equation takes the form;

$$P_L(\mathbf{r},t) = \frac{\varepsilon_0}{2\pi}\int_{-\infty}^{+\infty}\int_{-\infty}^{+\infty} \tilde{\chi}_{xx}^{(1)}(\omega)\tilde{E}(\mathbf{r},\omega-\omega_0)\exp\left[-i(\omega-\omega_0)t\right]d\omega, \tag{3.52}$$

The nonlinear response $\mathbf{P}_{\mathrm{NL}}$ is assumed to be instantaneous. Using the relations given in Appendix-A nonlinear polarization takes the form as

$$P_{NL}(\mathbf{r},t) \approx \varepsilon_0\varepsilon_{NL}E(\mathbf{r},t), \tag{3.53}$$

where ε_{NL} is nonlinear contribution to the dielectric constant, defined as

$$\varepsilon_{NL} = \frac{3}{4}\chi_{xxxx}^{(3)}\left|E(\mathbf{r},t)\right|^2. \tag{3.54}$$

Using (3.48), (3.52) and (3.53) into equation (3.46) and taking the Fourier transform;

$\tilde{E}(r,\omega-\omega_0)$ satisfies the Helmholtz equation

$$\nabla^2\tilde{\mathbf{E}} + \varepsilon(\omega)k_0^2\tilde{\mathbf{E}} = 0, \tag{3.55}$$

where $k_0 = \omega/c$ and $\varepsilon(\omega)$ is the dielectric constant given as

$$\varepsilon_0(\omega) = 1 + \tilde{\chi}_{xx}^1 + \frac{3}{4}\tilde{\chi}_{xxxx}^3\left|E(\mathbf{r},t)\right|^2. \tag{3.56}$$

Helmholtz equation and can be solved by using the method of separation of variables

$$\tilde{E}(\mathbf{r},\omega-\omega_0) = F(x,y)\tilde{E}(z,\omega-\omega_0)e^{i\beta_0 z}. \tag{3.57}$$

where $\tilde{E}(z,\omega-\omega_0)$ is a slowly varying function of *z* and *F(x, y)* is a function which corresponds to the transverse electric modes in the (x, y) plane if the z-axis is identical to the propagation direction.

Hence,

$$\frac{1}{F}\left(\frac{\partial^2 F}{\partial x^2}+\frac{\partial^2 F}{\partial y^2}\right)+\varepsilon(\omega)k_0^2=\frac{1}{\tilde{E}} \tag{3.58}$$

Making all constants match in Equation (3.58), equation takes the form as

$$\frac{\partial^2 F}{\partial x^2}+\frac{\partial^2 F}{\partial y^2}+\left[\varepsilon_0(\omega)k_0^2-\bar{\beta}^2\right]F=0, \tag{3.59}$$

$$\frac{\partial^2 \tilde{E}}{\partial z^2}+2i\beta_0\frac{\partial \tilde{E}}{\partial z}+\left[\bar{\beta}^2-\beta_0^2\right]\tilde{E}=0. \tag{3.60}$$

where $\bar{\beta}$ is the wave number and it is determined by solving the eigenvalue equation.

Due $\bar{E}(z,\omega)$ is a slowly varying function of *z*, the second derivative can be neglected. The eigenvalue $\bar{\beta}$ can be written as

$$\bar{\beta}(\omega)=\beta(\omega)+\Delta\beta, \tag{3.61}$$

where $\Delta\beta$ is a perturbation term and $\beta(\omega)$ is the frequency dependent mode propagation constant. Thus,

$$\frac{\partial \tilde{E}}{\partial z}-\frac{i}{2}\left\{\left[\beta(\omega)^2+2\beta(\omega)\Delta\beta\right]\frac{1}{\beta_0}-\beta_0\right\}\tilde{E}=0. \tag{3.62}$$

Expanding $\beta(\omega)$ in a Taylor-series around the carrier frequency ω_0 (Appendix-E) and neglecting the terms that are higher than second order such as $\beta_1\Delta\beta$ and $\beta_2\Delta\beta$. Thus, we may obtain the following equation in the Fourier space;

$$\frac{\partial \tilde{E}}{\partial z}-i\beta_1(\omega-\omega_0)\tilde{E}-\frac{i}{2}\beta_2(\omega-\omega_0)^2\tilde{E}-i\beta_0\Delta\beta\tilde{E}=0. \tag{3.63}$$

Combining Equation (3.61) and (3.62) and taking inverse Fourier transform;

$$\mathrm{F}^{-1}\left\{(\omega-\omega_0)\tilde{E}(z,\omega-\omega_0)\right\}=i\frac{\partial E(z,t)}{\partial t}, \tag{3.64}$$

and

$$\mathrm{F}^{-1}\left\{(\omega-\omega_0)^2\tilde{E}(z,\omega-\omega_0)\right\}=-\frac{\partial^2 E(z,t)}{\partial t^2}. \tag{3.65}$$

Following equation is achieved which defines the pulse propagation in optical fibers

$$\frac{\partial E}{\partial z}+\beta_1\frac{\partial E}{\partial t}+\frac{i\beta_2}{2}\frac{\partial^2 E}{\partial t^2}-i\Delta\beta E=0. \tag{3.66}$$

The term with $\Delta\beta$ includes the effect of fiber loss and nonlinearity.

$$\Delta\beta=-\frac{\alpha}{2}+i\gamma\left|E\right|^2, \tag{3.67}$$

where γ is the nonlinear coefficient defined by

$$\gamma=\frac{n_2\omega_0}{c\mathrm{A}_{\mathrm{eff}}}, \tag{3.68}$$

A_{eff} is the effective core area in which is inversely proportional to the nonlinearity.

n_2 is the so-called nonlinear refractive index which perturbs the linear index at higher intensities $n=n_0+n_2I$ (Appendix-C).

The effective core area is given in the form of

$$A_{\mathrm{eff}}=\frac{\left[\int_{-\infty}^{+\infty}\int\left|F(x,y)\right|^2\mathrm{d}x\mathrm{d}y\right]^2}{\int_{-\infty}^{+\infty}\int\left|F(x,y)\right|^4\mathrm{d}x\mathrm{d}y}. \tag{3.69}$$

where F(x, y) is the transverse mode field distribution that can be obtained from the eigenvalue equation. Making a variable transformation with

$$T=t-\frac{z}{v_g}=t-\beta_1 z, \tag{3.70}$$

The obtained equation is called Nonlinear Schrödinger Equation (NLSE) as follows;

$$\frac{\partial E(z,T)}{\partial z}=-\frac{\alpha}{2}E-\frac{i\beta_2}{2}\frac{\partial^2 E}{\partial T^2}+i\gamma\left|E\right|^2E \tag{3.71}$$

or

$$i\frac{\partial A}{\partial z}+\frac{i\alpha}{2}A-\frac{\beta_2}{2}\frac{\partial^2 A}{\partial T^2}+\gamma\left|A\right|^2 A=0. \tag{3.72}$$

The nonlinear term of the NLSE is $\gamma\left|A\right|^2 A$ .When the three-channel scenario is taken into consideration, i.e.:

$$A=A_1+A_2+A_3$$

The nonlinear term can be extended as:

$$\begin{aligned}
\left|A\right|^2 A &= A_1A_1^*A_1+A_1A_1^*A_2+A_1A_1^*A_3+A_1A_2^*A_1+A_1A_2^*A_2+A_1A_2^*A_3+A_1A_3^*A_1+A_1A_3^*A_2+A_1A_3^*A_3\\
&\quad+A_2A_1^*A_1+A_2A_1^*A_2+A_2A_1^*A_3+A_2A_2^*A_1+A_2A_2^*A_2+A_2A_2^*A_3+A_2A_3^*A_1+A_2A_3^*A_2+A_2A_3^*A_3\\
&\quad+A_3A_1^*A_1+A_3A_1^*A_2+A_3A_1^*A_3+A_3A_2^*A_1+A_3A_2^*A_2+A_3A_2^*A_3+A_3A_3^*A_1+A_3A_3^*A_2+A_3A_3^*A_3\\
&=\left|A_1\right|^2A_1+\left|A_2\right|^2A_2+\left|A_3\right|^2A_3+2\left|A_1\right|^2A_2+2\left|A_1\right|^2A_3+2\left|A_2\right|^2A_1+2\left|A_2\right|^2A_3\\
&\quad+2\left|A_3\right|^2A_1+2\left|A_3\right|^2A_2+A_1^2A_2^*+A_1^2A_3^*+A_2^2A_1^*+A_2^2A_3^*+A_3^2A_1^*+A_3^2A_2^*\\
&\quad+2A_1A_2A_3^*+2A_1A_3A_2^*+2A_2A_3A_1^*\\
&=\underbrace{\left|A_1\right|^2A_1+\left|A_2\right|^2A_2+\left|A_3\right|^2A_3}_{\text{SPM}}\\
&\quad+\underbrace{2\left|A_1\right|^2A_2+2\left|A_1\right|^2A_3+2\left|A_2\right|^2A_1+2\left|A_2\right|^2A_3+2\left|A_3\right|^2A_1+2\left|A_3\right|^2A_2}_{\text{XPM}}\\
&\quad+\underbrace{A_1^2A_2^*+A_1^2A_3^*+A_2^2A_1^*+A_2^2A_3^*+A_3^2A_1^*+A_3^2A_2^*}_{\text{degenerate FWM}}+\underbrace{2A_1A_2A_3^*+2A_1A_3A_2^*+2A_2A_3A_1^*}_{\text{non-degenerate FWM}}
\end{aligned}$$

4. NUMERICAL ALGORITHM AND SIMULATIONS

4.1 Numerical method to solve NLSE

Nonlinear Schrödinger Equation (3.71) is used to analyze the different physical phenomena encountered when ultrashort pulses propagate through dispersive and nonlinear fibers. Since it is difficult to obtain the analytical solution of the equation, different approaches have been developed to determine the numerical solution.

Split Step Fourier Method (SSFM) is the most effective and widely used method to find the numerical solution of NLS equation. Split-Step Fourier method considers the effects of attenuation, dispersion and nonlinearity over suitable small distances of the fiber (from z to z+dz) where z is a running variable over the entire length of the fiber, and dz is step size.

In SSFM, the given fiber length is conceptually divided into a large number of steps or segments. The propagation of the optical pulse is executed for each segment sequentially divided by linear and nonlinear parts. The nonlinear term is solved in time domain, while the dispersion term (linear term) is solved in the frequency domain using fast Fourier transform (FFT).

The NLSE given in equation (3.71) describes the effects of fiber attenuation, dispersion and nonlinearities;

$$\frac{\partial A(z,t)}{\partial z} = -\frac{\alpha}{2}A(z,t) - j\frac{\beta_2}{2}\frac{\partial^2 A(z,t)}{\partial t^2} + j\gamma\left|A(z,t)\right|^2.A(z,t) \tag{4.1}$$

In order to solve NLS equation by the SSF method, following functional differential equation is written by separating linear and nonlinear parts as:

$$\frac{\partial A(z,t)}{\partial z} = [L+N].A(z,t) \tag{4.2}$$

where ***L*** represents linear part and ***N*** represents the nonlinear part respectively.

$$L = -\frac{\alpha}{2} - j\frac{\beta_2}{2}\frac{\partial^2}{\partial t^2} \tag{4.3}$$

$$N = j\gamma\left|A(z,t)\right|^2 \tag{4.4}$$

Integrating along **z** using a small space interval **Δz** , the solution can be written in the form of

$$A(z+\Delta z,t)=\exp(\Delta z\left[L+N\right]).A(z,t) \tag{4.5}$$

The effects of the linear operator implemented in frequency domain. The time derivatives of linear operator are replaced by $(j\omega)^n$ and thereby converted to Fourier Space where *n* is the order of the derivative.

4.2 Symmetric Split Step Fourier Method

The symmetric split step Fourier method (S-SSFM) subdivides the global propagation distance into steps of length and supposes that the effects of dispersion and nonlinearity act independently along each step. Effects of nonlinearity are inserted at the middle of each step $(\Delta z/2)$ of the fiber. Schematic illustration of this method is shown in Figure 4.1 [14].

$$A(z+\Delta z,t)\approx e^{\frac{h}{2}L}e^{hN}e^{\frac{h}{2}L}A(z,t) \tag{4.6}$$

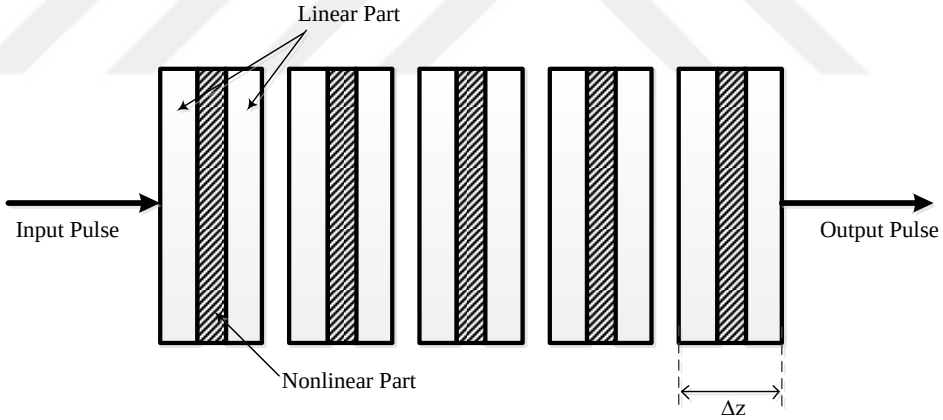

Figure 4.1: Schematic view of SSFM process.

Equation (4.6) can be approximated as,

$$A(z+\Delta z,t)=\exp\left[\frac{\Delta z}{2}L\right].\exp\left[\int_{z}^{z+\Delta z}N(z)dz\right].\exp\left[\frac{\Delta z}{2}L\right]A(z,t) \tag{4.7}$$

where

$$\int_{z}^{z+\Delta z}N(z)dz\cong\frac{\Delta z}{2}\left[N(z)+N(z+\Delta z)\right] \tag{4.8}$$

The symmetric split-step Fourier method (S-SSFM) which is derived from the fact that the dispersive and nonlinear operators do not commute thus, It can be shown that the global relative error of the symmetric split-step Fourier method (S-SSFM) is $O(\Delta z)^2$ where Δz is the spatial step size. Linear term is solved in frequency domain using FFT routines whereas the nonlinear term is solved in time domain.

For a fiber with length z, the number of steps is $(z/\Delta z)$.

In every step of iteration amplitude (A) moves to the next step governed by following algortihm

$A_k = A(k\Delta z, t)$ where $k = 0, \ldots, h$

$$A_1 = IFFT\left\{ e^{\frac{\Delta z}{2}L} \left[FFT(A_k) \right] \right\}$$

$$A_2 = e^{\Delta z.N} A_1$$

$$A_{k+1} = IFFT\left\{ e^{\frac{\Delta z}{2}L} \left[FFT(A_2) \right] \right\} \qquad (4.9)$$

The method proceeds as follows:

STEP-1: Take $N \equiv 0$ and solve Linear part in frequency domain as

$$F\left[\frac{\partial A(z,t)}{\partial z} = -\frac{\alpha}{2} A(z,t) - j\frac{\beta_2}{2} \frac{\partial^2 A(z,t)}{\partial t^2} + j\gamma \left| A(z,t) \right|^2 . A(z,t) \right]$$

Let

$$-\frac{\alpha}{2} A(z,t) - j\frac{\beta_2}{2} \frac{\partial^2 A(z,t)}{\partial t^2} = \boldsymbol{B}$$

taking the fourier transform of dispersive term

$$\tilde{\boldsymbol{B}} = -\frac{\alpha}{2} \tilde{A} - j\frac{\beta_2}{2} \omega^2 \tilde{A}$$

where the linear operator can be implemented in the frequancy-domain by using the

correspondence $\frac{\partial^2}{\partial t^2} = (i\omega)^2$

$$\tilde{A}(z+\Delta z/2,\omega)=e^{\tilde{\boldsymbol{B}}(\Delta z/2)}A(0,\omega)$$

$$F^{-1}\left[\tilde{A}(z+\Delta z/2,\omega)\right]=A(z+\Delta z/2,t)=A_1$$

STEP-2: Take $L\equiv 0$ and solve Nonlinear part in time domain as

$$\frac{\partial A(z+\Delta z,t)}{\partial z}=j\gamma\left|A(z,t)\right|^2.A(z,t)$$

$$A(z+\Delta z,t)=e^{j\gamma|A(z,t)|^2\Delta z}A_1$$

$$F^{-1}\left[\tilde{A}(z+\Delta z,t)\right]=A(z+\Delta z,t)=A_2$$

STEP-3: Take $N\equiv 0$ once more and solve Linear part in frequency domain as

$$-\frac{\alpha}{2}A(z,t)-j\frac{\beta_2}{2}\frac{\partial^2 A(z,t)}{\partial t^2}=\boldsymbol{B}$$

taking the fourier transform

$$\tilde{\boldsymbol{B}}=-\frac{\alpha}{2}\tilde{A}-j\frac{\beta_2}{2}\omega^2\tilde{A}$$

where $\dfrac{\partial^2}{\partial t^2}=\omega^2$

$$\tilde{A}(z+\Delta z/2,\omega)=e^{\tilde{\boldsymbol{B}}(\Delta z/2)}A_2$$

$$F^{-1}\left[\tilde{A}(z+\Delta z/2,\omega)\right]=A(z+\Delta z/2,t)=A_{h+1}$$

Algorithm terminates at the h-th iteration and A_h is used to plot output shape of the pulse. Detailed algorithm of S-SSFM and related Matlab code are given in Appendix-F.

The initial pulse width $A_0=A(0,t)$ is chosen as Gaussian pulse as given in Appendix-D.

4.3 Simulations

In this section a Matlab based simulation software is presented according to mathematical model given in Section 4.1.

Selected simulation parameters are
Center wavelength: 1550 nm
Effective core area: 78 μm^2
Fiber attenuation: 0.22 dB/km
Dispersion parameter: 17 ps/nm.km
Nonlinear refractive index: 2.68
Input power: 0.5 mW
Nominal Channel spacing: 0.8 nm (100 GHz)

There are many factors which have significant influence on the magnitude of FWM products. Some of these factors are channel spacing and dispersion parameter. Different types of fibers have different dispersion parameters. Various typical values of dispersion parameter D (β_2= …) are considered. D is inversely proportional to the FWM component power.

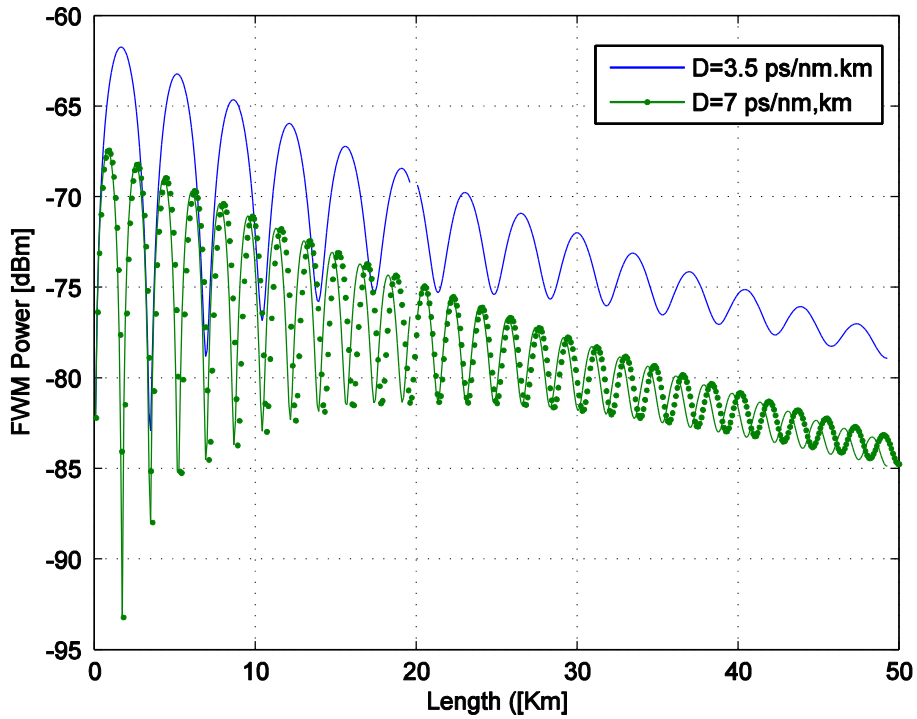

Figure 4.2: FWM power change along with the fiber length with respect to different dispersion parameters.

In Figure 4.2 effect of channel spacing on FWM Efficiency is shown for four different values of fiber dispersion. Increasing fiber dispersion will decrease FWM efficiency. For low dispersion fibers another factor that increases the FWM power is DWDM signal channel spacing. In this case FWM efficiency becomes larger even for the large channel spacing values.

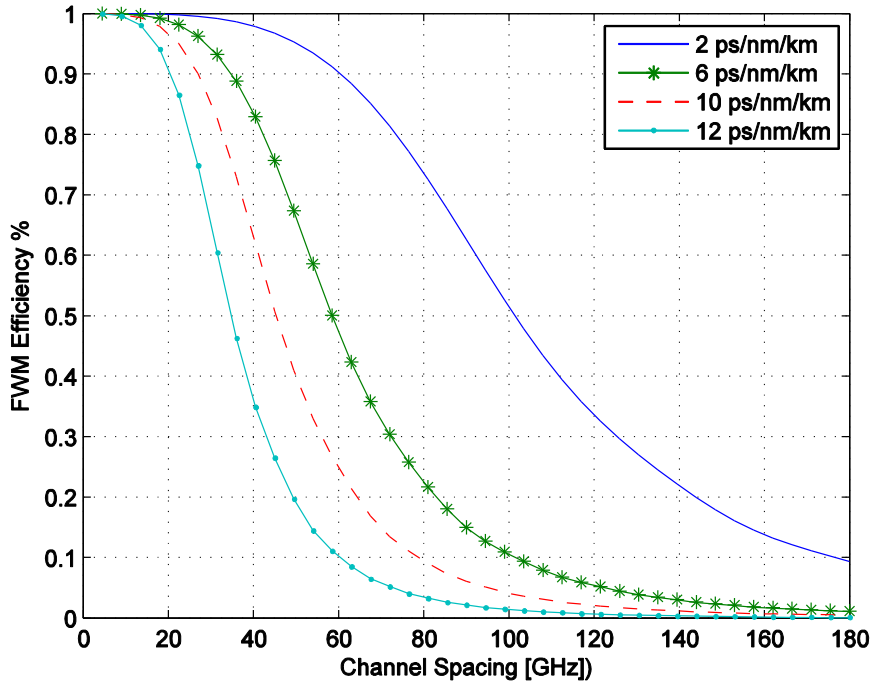

Figure 4.3 : Variation of FWM Efficiency with different channel spacing for different dispersion parameters.

In Figure 4.4, different FWM component power are presented for different types of fibers with parameters given in Table 4.1.

Table 4.1: Characteristics of different types of optical fibers.

Fiber Type	$A_{eff}\ (\mu m)^2$	*D (ps/nm.km)*	*α(dB/km)*	$\gamma\ (W^{-1}km)$
SMF	80	17	0.2	2.5
NZDSF	50	-3	0.23	3.9
DCF	20	-80	0.29	3

Maxima of the FWM power occurs when $\Delta\beta.\frac{L}{2} = n.\pi$, where n is an arbitrary integer due to the phase mismatch between propagating signals. Figure 4.4 shows that power of FWM compoenets are effected by fiber parameters and variation in channel spacing. Considering

FWM efficiency equation, minimum values of the FWM power occurs every $2\pi/\Delta\beta$ meter.

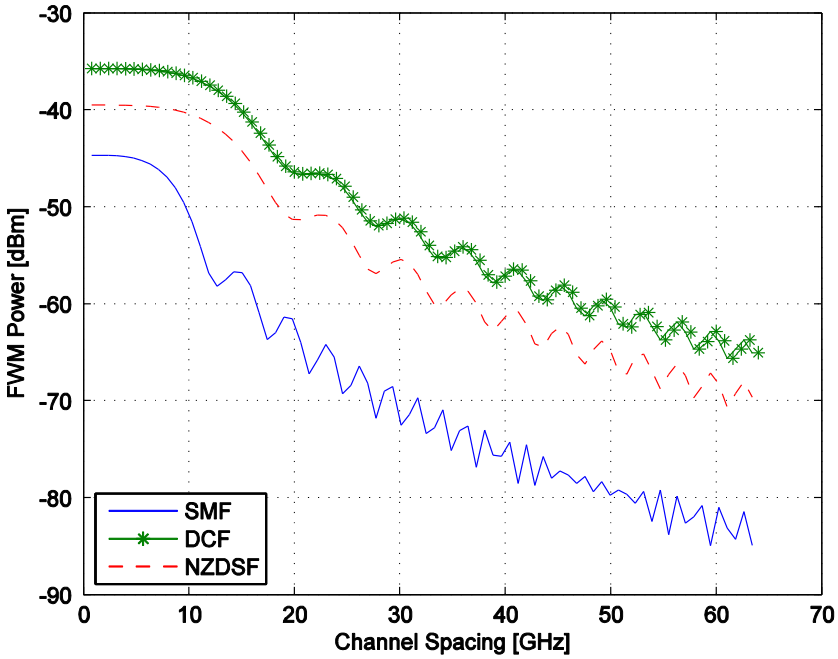

Figure 4.4: Variation of FWM Power with different channel spacing for different types of fiber.

As can be seen from the simulation outputs presented in the Figure 4.5, FWM power is dependent on channel input powers and increases as channel power increased. FWM component power saturates at some distance propagated along the fiber.

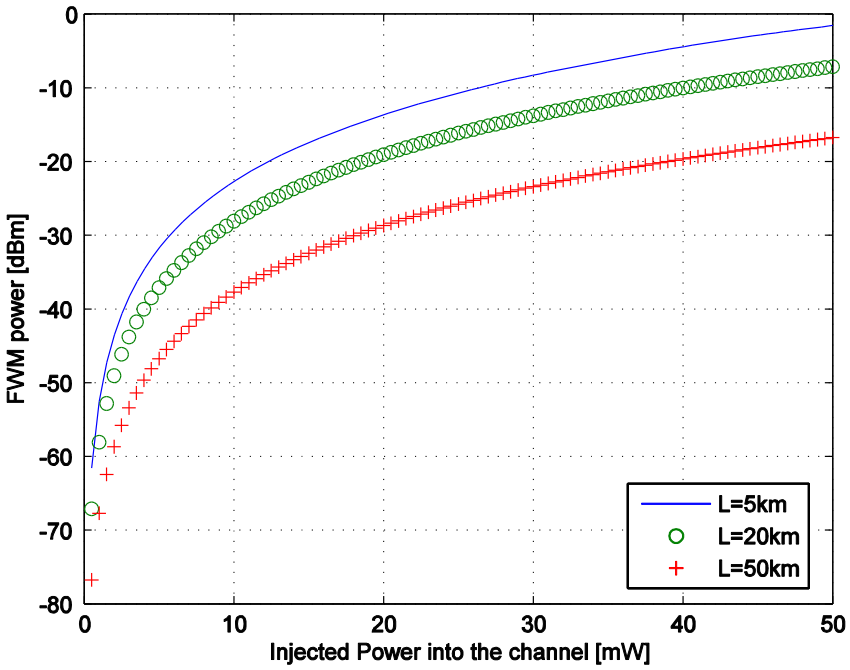

Figure 4.5: FWM Noise Power change with Injected power.

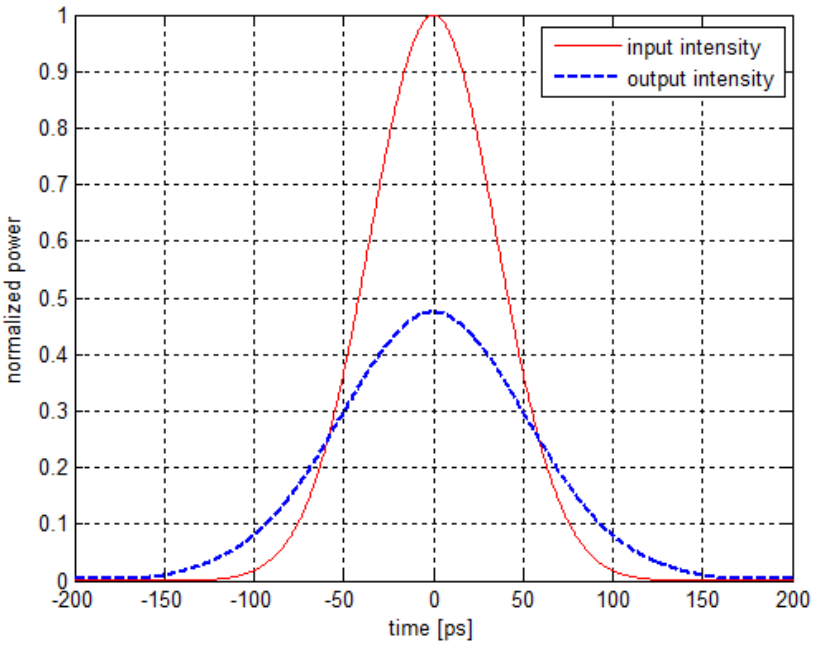

Figure 4.6: Intensities at input and output.

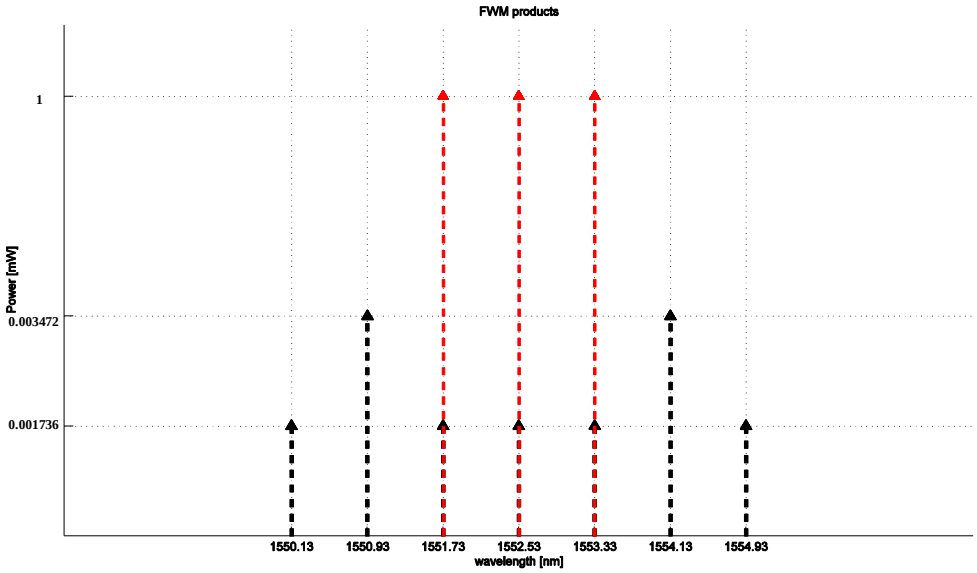

Figure 4.7: Produced FWM components for equidistant 3 channel DWDM system.

4.4 Results

In this thesis, effect of FWM in a wavelength division multiplexed (WDM) optical communication system has investigated. Simulations demonstrate that efficiency of FWM effect is dependent on type of fiber, fiber length, channel input power and channel spacing.

As the number of channels increases, number of FWM components also increases exponentially. Therefore designing system with a narrower wavelength produces more FWM terms on the same signal channel which leads to degradation of original signals and interference between them. In order to avoid this degradation in the performance of the system unequal channel spacing scheme can be implemented. Thereby, it's possible to avoid some of the produced FWM terms to coincide with original channels. But this design strategy leads to a trade-off between limiting FWM effects and efficient use of available large bandwidth of the fiber. Dispersion management in the system design is another limiting factor which increases FWM efficiency. A signal propagating with constant group velocity and constant phase along the fiber leads to increased FWM effect which has its greatest value in the zero dispersion wavelength region.

4.5 Future Work

Some of the techniques to reduce FWM effects are proposed in the previous sections. Using unequal channel spacing and also extending the number of channels requires additional optical bandwidth. Polarization multiplexing of DWDM channels is an alternative technique to obtain higher spectral efficiency with an beneficial improvement in reducing of channel spacing.

It has been experimentally resulted that the reduction of FWM power in WDM systems is possible with arranging the signal lights having orthogonal state of polarization. Using polarization-multiplexed schemes is particularly helpful to reduce of nonlinear crosstalk effect caused by FWM in DWDM systems. Applying the polarization state of each DWDM channel orthogonal to the adjacent one along the fiber provides a FWM product suppression factor of 4. Since, practically, the state of polarization cannot be maintained constant along the fiber especially for long-haul systems DGD varies randomly. When system differential group-delay (DGD) is smaller than $1/(4\Delta f)$, where Δf is the channel-spacing, it's possible to get a significant improvement in system performance. However, in the regime that this condition is satisfied, even a small amount of PMD reduce helps to suppression of nonlinear crosstalk of FWM [15,16].

Recent advences in higher order modulation formats made implementing available of higher data rates 40 Gbit/s and 100 Gbit/s. In practice linear effects such as Chromatic Dispersion, Polarization-Mode Dispersion and nonlinear impairments of fiber are compensated with passive optical components in optical side of the DWDM systems. In order to achieve higher bit rates with properly suppressed linear and nonlinear effects, coherent detection techniques are developed along with the digital signal processing which provides a significant improvement in spectral efficiency. In coherent detection mechanism, complex field of the received signal is fully recovered interfering with a hybrid local oscillator while the linear impairments are compensated along with the digital filters. Electronic dispersion compensation and digital backward propagation are some of the coherent detection techniques [17-19].

REFERENCES

[1] **Saleh, A. A.**, **& Simmons, J. M.,** (2011). Technology and architecture to enable the explosive growth of the internet. *Communications Magazine, IEEE*, 49(1), 126-132.

[2] **Agrawal, G.** (2002). *Fiber-Optic Communication Systems* (Third Edition), Wiley.

[3] **Brackett, C. A.,** (1990). Dense wavelength division multiplexing networks: Principles and applications. *Selected Areas in Communications, IEEE Journal on*, 8(6), 948-964.

[4] **Dixit, S., & Ye, Y.,** (2001). Streamlining the Internet-fiber connection. *Spectrum IEEE*, 38(4), 52-57.

[5] **Yu, T., Golovchenko, E. A., Pilipetskii, A. N., and Menyuk, C. R.,** (1997). Dispersion-managed soliton interactions in optical fibers. *Optical letters*, 22(11), 793-795.

[6] **Murakami, M., Matsuda, T., Maeda, H., & Imai, T.,** (2000). Long-haul WDM transmission using higher order fiber dispersion management. *Journal of Lightwave Technology*, 18(9), 1197.

[7] **Agrawal, G.** (2007). *Nonlinear Fiber Optics* (Fourth Edition), Academic Press.

[8] **Forghieri, F., Tkach, R. W., and Chraplyvy, A. R.,** (1997). Fiber nonlinearities and their impact on transmission systems. *Optical Fiber Telecommunications IIIA*, Academic Press.

[9] **Inoue, K.,** (1992). Four-wave mixing in an optical fiber in the zero-dispersion wavelength region. *Lightwave Technology, Journal of*, 10(11), 1553-1561.

[10] **Tkach, R. W., Chraplyvy, A. R., Forghieri, F., Gnauck, A. H.** (1995). Four-photon mixing and high-speed WDM systems. *Lightwave Technology, Journal of*, 13(5), 841-849.

[11] **Harboe, P. B., da Silva, E., & Souza, J. R.,** (2008). Analysis of FWM penalties in DWDM systems based on G.652, G.653, and G.655 optical fibers. In *Proceedings of World Academy of Science, Enginnering and Technology*, (Vol. 35).

[12] **Chomycz, B.** (2009). *Planning Fiber Optics Networks*, McGraw-Hill Professional.

[13] **Ramaswami, R.**, **Sivarajan, K. N., & Sasaki, G. H.** (2009). *Optical Networks: a practical perspective.* Morgan Kaufmann.

[14] **Strang, G.,** (1968). On the construction and comparison of difference schemes, *SIAM Journal on Numerical Analysis*, 5(3), 506-517.

[15] **Inoue, K.,** (1991). Arrangement of orthogonal polarized signals for suppressing fiber four-wave mixing in optical multichannel transmission systems, *Photonics Technology Letters, IEEE*, 3(6), 560-563.

[16] **Hansryd, J., Sunnerud, H., Andrekson, P. A., & Karlsson, M.** (2000). Impact of PMD on four-wave-mixing-induced crosstalk in WDM systems. *Photonics Technology Letters, IEEE*, 12(9), 1261-1263.

[17] **Savory, S. J., Gavioli, G., Killey, R. I., & Bayvel, P.** (2007). Electronic compensation of chromatic dispersion using a digital coherent receiver. *Opt. Express*, 15(5), 2120-2126.

[18] **Li, G.** (2009). Recent advances in coherent optical communication. *Adv. Opt. Photon*, *1*(2), 279-307.

[19] **Okoshi, T., & Kikuchi, K.** (1988). *Coherent optical fiber communications*. (Vol. 3). Springer.

APPENDIX-A

NONLINEAR SUSCEPTIBILITY

The components of polarization vector $\vec{P}$ can be expressed as

$$\frac{1}{\varepsilon_0} P_i = \sum_j \chi_{ij}^{(1)} E_j + \sum_{j,k} \chi_{ijk}^{(2)} E_j E_k + \sum_{j,k,l} \chi_{ijkl}^{(3)} E_j E_k E_l + \cdots \quad \text{(A.1)}$$

Optical fiber material (SiO_2) is isotropic (at λ region of interest). Therefore the electric susceptibility tensors should also be isotropic.

When represented in a Cartesian frame the most general isotropic tensors of rank 0-4 are as follows: [Ref. R.E. Hunt Mathematical Methods II, pg.60]

Rank 0: All scalars are isotropic.

Rank 1: There are no non-zero isotropic vectors.

Rank 2: $\chi_{ij}^{(1)} = \lambda \delta_{ij}$ where λ is any scalar.

Rank 3: $\chi_{ijk}^{(3)} = \lambda \varepsilon_{ijk}$.

Rank 4: $\chi_{ijkl}^{(4)} = \lambda \delta_{ij}\delta_{kl} + \mu \delta_{ik}\delta_{jl} + \nu \delta_{il}\delta_{jk}$ where $\lambda,\ \mu,\ \delta$ are scalars.

$\delta_{ij} = \begin{cases} 1 & \text{if } i = j \\ 0 & \text{if } i \neq j. \end{cases}$ the Kronecker's delta tensor

$\varepsilon_{ijk} = \begin{cases} 1 & for \quad (1,2,3),(2,3,1) \text{ and } (3,1,2) \\ -1 & for \quad (1,3,2),(2,1,3) \text{ and } (3,2,1) \\ 0 & else \end{cases}$ the permutation tensor

Isotropic tensor is one whose components are the same in all frames.

A tensor $T_{ijk\ldots}$ is said to be symmetric in a pair of indices (say *i j*) if $T_{ijk\ldots} = T_{jik\ldots}$ or anti-symmetric if it satisfies $T_{ijk\ldots} = -T_{jik\ldots}$.

Thus for isotropic case, $\chi^{(2)}$ is anti-symmetric whereas $\chi^{(1)}$ and $\chi^{(3)}$ are symmetric.

Optical fibers are represented with isotropic and symmetric tensors here.

$$\frac{1}{\varepsilon_0} P_i = \underline{\chi}^{(1)} \delta_{ij} E_j + \underline{\chi}^{(3)} \delta_{ij} \delta_{kl} E_l E_k E_j \qquad \text{(A.2)}$$

where $\underline{\chi}$'s are scalars and Einstein convention is used [summation over repeated indices]

Assume that

$\underline{\chi}^{(3)} = \lambda$ and $\mu = \nu = 0$

$$\chi_{ijkl} E_l = (\chi_{111} + \chi_{221} + \chi_{331}) E_1 + (\chi_{112} + \chi_{222} + \chi_{332}) E_2 + (\chi_{113} + \chi_{223} + \chi_{333}) E_3$$

$$\chi_{ijkl} E_l E_k = (\chi_{11} + \chi_{22} + \chi_{33})[E_1 E_1 + E_2 E_2 + E_3 E_3]$$

$$\chi_{ijkl} E_l E_k E_j = \chi |E|^2 E \qquad \text{(A.3)}$$

For an x-polarized wave we have

$$\frac{1}{\varepsilon_0} P_x^{NL} = \underline{\chi}^{(3)} |E_x|^2 E_x$$

(A.4)

where superscript NL stands for nonlinear part of polarization. **Linear part** being simply

$$P_L = \varepsilon_0 \underline{\chi}^{(1)} E_X \qquad \text{(A.5)}$$

the isotropy of the medium makes $\chi^{(3)}$ is invariant under any rotational transformation.

$\chi_{1111} = \chi_{2222} = \chi_{3333}$

$\chi_{1212} = \chi_{1313}$

Following this same logic, all $\chi^{(3)}_{iijj}$ are the same for $i \neq j$ all $\chi^{(3)}_{ijji}$ are the same for $i \neq j$, and all $\chi^{(3)}_{ijij}$ are the same for $i \neq j$.

Thus,

$\chi_{1111} = \chi_{2222} = \chi_{3333}$

$\chi_{1122} = \chi_{1133} = \chi_{2211} = \chi_{2233} = \chi_{3311} = \chi_{3322}$

$\chi_{1212} = \chi_{1313} = \chi_{2323} = \chi_{2121} = \chi_{3131} = \chi_{3232}$

$\chi_{1221} = \chi_{1331} = \chi_{2112} = \chi_{2332} = \chi_{3113} = \chi_{3223}$

Therefore nonlinear part can be derived by

$$\frac{1}{\varepsilon_0} P_i = \sum_j \chi_{ij}^{(1)} E_j + \sum_{j,k} \chi_{ijk}^{(2)} E_j E_k + \sum_{j,k,l} \chi_{ijk}^{(3)} E_j E_k E_l + \cdots$$

$$P = \varepsilon_0 \chi^{(1)} E + \overbrace{\varepsilon_0 \chi^{(2)} E^2}^{0} + \varepsilon_0 \chi^{(3)} E^3 + \cdots \tag{A.6}$$

$$E = E_0 \cos(\omega t - kz)$$

$$P = \varepsilon_0 \chi^{(1)} E_0 \cos(\underbrace{\omega t - kz}_{\alpha}) + \overbrace{\varepsilon_0 \chi^{(2)} {E_0}^2 \cos^2(\underbrace{\omega t - kz}_{\alpha})}^{0} + \varepsilon_0 \chi^{(3)} E^3 \cos^3(\underbrace{\omega t - kz}_{\alpha}) + \cdots$$

Using trigonometric relations;

$$\cos^2(\alpha) = \frac{1}{2}(1 + \cos 2\alpha)$$

$$\cos^3(\alpha) = \frac{1}{4}(\cos 3\alpha + 3\cos\alpha) \tag{A.7}$$

We obtain;

$$P = \varepsilon_0 \chi^{(1)} E_0 \cos\alpha + \varepsilon_0 \chi^{(2)} {E_0}^2 \frac{1}{2}(1 + \cos 2\alpha) + \varepsilon_0 \chi^{(3)} {E_0}^3 \frac{1}{4}(\cos 3\alpha + 3\cos\alpha)$$

$$\frac{1}{\varepsilon_0} P = \chi^{(1)} E_0 \cos\alpha + \overbrace{\frac{1}{2}\chi^{(2)} {E_0}^2}^{0} + \overbrace{\frac{1}{2}\chi^{(2)} {E_0}^2 \cos 2\alpha}^{0} + \frac{1}{4}\chi^{(3)} {E_0}^3 \cos 3\alpha + \frac{3}{4}\chi^{(3)} {E_0}^3 \cos\alpha \tag{A.8}$$

$$\frac{1}{\varepsilon_0} P = \chi^{(1)} E_0 \cos(\omega t - kz) + \overbrace{\frac{1}{4}\chi^{(3)} {E_0}^3 \cos 3(\omega t - kz)}^{0} + \frac{3}{4}\chi^{(3)} {E_0}^3 \cos(\omega t - kz)$$

$$P = \varepsilon_0 \chi^{(1)} E_0 \cos(\omega t - kz) + \frac{3}{4}\varepsilon_0 \chi^{(3)} {E_0}^3 \cos(\omega t - kz)$$

APPENDIX-B

NONLINEAR POLARIZATION IN FWM

To understand the effects of four-wave mixing, consider a WDM signal that is the sum of *n* monochromatic plane waves. Thus the electric field of this signal can be written as

$$E(\mathbf{r},t)=\sum_{i=1}^{n}E_i\cos(\omega_i t-\beta_i z) \tag{B.1}$$

$$\begin{aligned}P_{NL}(\mathbf{r},t)&=\varepsilon_0\chi^{(3)}\sum_{i=1}^{n}\sum_{j=1}^{n}\sum_{k=1}^{n}E_i\cos(\omega_i t-\beta_i z)E_j\cos(\omega_j t-\beta_j z)E_k\cos(\omega_k t-\beta_k z)\\&=\frac{3\varepsilon_0\chi^{(3)}}{4}\sum_{i=1}^{n}\left(E_i^{\,2}+2\sum_{j\neq i}E_iE_j\right)E_i\cos(\omega_i t-\beta_i z)\end{aligned} \tag{B.2}$$

$$+\frac{\varepsilon_0\chi^{(3)}}{4}\sum_{i=1}^{n}E_i^3\cos(3\omega_i t-3\beta_i z) \tag{B.3}$$

$$+\frac{3\varepsilon_0\chi^{(3)}}{4}\sum_{i=1}^{n}\sum_{j\neq i}E_i^2E_j\cos((2\omega_i-\omega_j)t-(2\beta_i-\beta_j)z) \tag{B.4}$$

$$+\frac{3\varepsilon_0\chi^{(3)}}{4}\sum_{i=1}^{n}\sum_{j\neq i}E_i^2E_j\cos((2\omega_i+\omega_j)t-(2\beta_i+\beta_j)z) \tag{B.5}$$

$$+\frac{6\varepsilon_0\chi^{(3)}}{4}\sum_{i=1}^{n}\sum_{j>i}\sum_{k>j}E_iE_jE_k \tag{B.6}$$

$$(\cos((\omega_i+\omega_j+\omega_k)t-(\beta_i+\beta_j+\beta_k)z)$$

$$+(\cos((\omega_i+\omega_j-\omega_k)t-(\beta_i+\beta_j-\beta_k)z) \tag{B.7}$$

$$+(\cos((\omega_i-\omega_j+\omega_k)t-(\beta_i-\beta_j+\beta_k)z) \tag{B.8}$$

$$+(\cos((\omega_i-\omega_j-\omega_k)t-(\beta_i-\beta_j-\beta_k)z)) \tag{B.9}$$

The terms (B.3), (B.5), and (B.6) can be neglected because of lack of phase matching. Under appropriate conditions, it is likely to approximately satisfy the phase-matching condition for the rest of the terms, which are all of the form

$\omega_i+\omega_j-\omega_k,\ i,j\neq k$ ($\omega_i,\ \omega_j$ not necessarily distinct)

For instance, if the wavelengths in the WDM system are closely distributed, or are distributed near the dispersion zero of the fiber, then β is nearly constant over these frequencies and the condition of phase-matching is nearly satisfied.

APPENDIX-C

RELATION BETWEEN NONLINEAR REFRACTIVE INDEX AND INTENSITY

In terms of nonlinear refractive index nonlinear part of polarization can be written as

$$P_x^{NL} \approx \varepsilon_0 \varepsilon_{NL} E \tag{C.1}$$

where

$$\varepsilon_{NL} = \frac{3}{4} \chi_{xxxx}^{(3)} |E|^2 \tag{C.2}$$

There are various effects that are resulting from degenerate four-wave mixing.

$$P_{NL} = \varepsilon_0 \chi^{(3)} E_1 E_2^* E_3 \tag{C.3}$$

Assume

$$E_1 = E_2 = E_3 = E$$

So the polarization becomes:

$$P_{NL} = \varepsilon_0 \chi^{(3)} |E|^2 E \tag{C.4}$$

Single-field degenerate four-wave mixing causes “self” effects.

Recall inhomogeneous wave equation:

$$\frac{\partial^2 E}{\partial z^2} - \frac{1}{{c_0}^2} \frac{\partial^2 E}{\partial t^2} = \mu_0 \frac{\partial^2 P}{\partial t^2} \tag{C.5}$$

the polarization envelope (the linear and nonlinear terms):

$$P = \varepsilon_0 \left[\chi^{(1)} E + \chi^{(3)} |E|^2 E \right] = \varepsilon_0 \left[\chi^{(1)} + \chi^{(3)} |E|^2 \right] E \tag{C.6}$$

Substituting the polarization into the wave equation (assuming slow variation in the envelope of E compared to $1/\omega$):

$$\frac{\partial^2 E}{\partial z^2} - \frac{1}{c_0^2} \frac{\partial^2 E}{\partial t^2} = \mu_0 \varepsilon_0 \left[\chi^{(1)} + \chi^{(3)} |E|^2 \right] \frac{\partial^2 E}{\partial t^2} \tag{C.7}$$

$$\frac{\partial^2 E}{\partial z^2} - \frac{\left[1 + \chi^{(1)} + \chi^{(3)}\left|E\right|^2\right]}{c_0^2}\frac{\partial^2 E}{\partial t^2} = 0 \quad \text{since} \quad \mu_0\varepsilon_0 = 1/c^2 \tag{C.8}$$

So the refractive index is:

$$n = \sqrt{1 + \chi^{(1)} + \chi^{(3)}\left|E\right|^2} \tag{C.9}$$

the usual refractive index (which we called as n_0) is:

$$n_0 = \sqrt{1 + \chi^{(1)}}$$

$$n = \sqrt{n_0^2 + \chi^{(3)}\left|E\right|^2}$$

$$= n_0\sqrt{1 + \chi^{(3)}\left|E\right|^2 / n_0^2} \tag{C.10}$$

Assume that the nonlinear term << n_0:

$$n \approx n_0\left[1 + \chi^{(3)}\left|E\right|^2 / 2{n_0}^2\right]$$

$$n \approx n_0\chi^{(3)}\left|E\right|^2 / 2n_0$$

since $I \propto \left|E\right|^2$

$$n \approx n_0 + n_2 I \tag{C.11}$$

Take $n_0 = 1.46$ and $n_2 = 3.2\times10^{-20}$ m^2/W. For the propagation of a mode carrying 100 mW of power in a SMF, for $A_{eff} = 50$ $\mu\mathrm{m}^2$, intensity becomes 2×10^9 W/m^2.

Change in refractive index due to the NL effect is

$$n_2 I = 6.4\times10^{-11}$$

This change in refractive index becomes very significant when thousands of km fiber lengths are used.

APPENDIX-D

GAUSSIAN BEAM AND PULSE

Gaussian Beam

It is crucial to know the propagation characteristics of laser beam in most laser applications. Generally, laser-beam propagation can be approximated by assuming that the laser beam has an ideal Gaussian intensity profile.

Many lasers emit beams with a Gaussian profile, in which case the laser is said to be operating on the fundamental transverse mode, or "**TEM$_{00}$** mode" of the laser's optical resonator. When refracted by a lens, a Gaussian beam is transformed into another Gaussian beam (characterized by a different set of parameters), which explains why Gaussian optics is a convenient, widespread model in laser optics.

The Gaussian beam is a radially symmetrical distribution whose electric field variation is given by the following equation:

$$E_s = E_0 e^{-(r/w_0)^2} \tag{D.1}$$

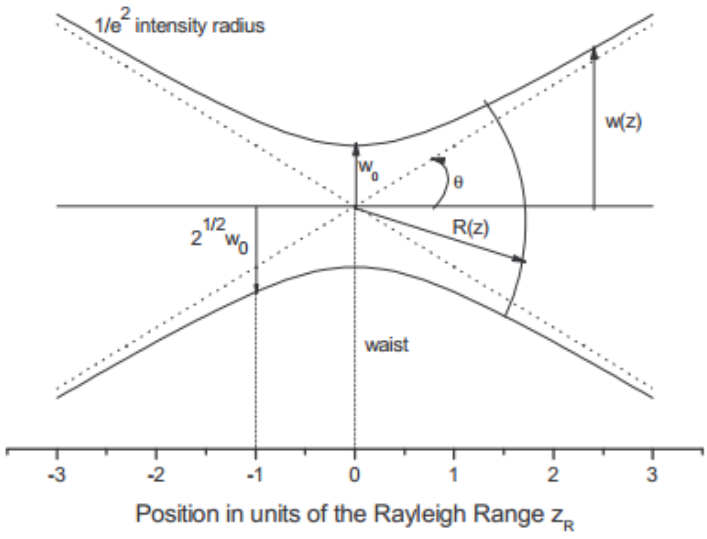

Figure D.1: Focus of Gaussian beam.

The beam radius *R(z)*has its minimum value w_0 at the waist (z=0), reaches $\sqrt{2}w_0$ at $z = \pm z_0$, and increases linearly with z for large z

where $\theta = w_0/z_0$

Consider x polarized wave in a weakly guiding single mode fiber.

The electric field ***E*** can be written in phasor form as

$$E_x = E_0 e^{-(r/w)^2} e^{-\frac{\alpha}{2}z} e^{j(\omega t - \beta z)} \tag{D.2}$$

We assume the beam waist parameter "*w*" and the attenuation constant "α" to be constant over DWDM band.

Let the power injected at the input (z=0) be ***P*** then

$$P = \frac{E_0^2}{z} \int_{S_\infty} e^{-2(r/w)^2} r dr d\varphi = E_0^2 B^2 \tag{D.3}$$

where $B^2 = \frac{\pi\omega}{2Z_0}$, $Z_0 = \sqrt{\frac{\mu_0}{\varepsilon_0}} \frac{1}{\sqrt{\varepsilon_r}}$

Thus we can write

$\Psi = E_x B$ with the understanding $\left|\Psi_{(0)}\right| = \sqrt{P}$

To eliminate the rapid variation we introduce

$\Psi = A e^{j[\omega_0 t - \beta(\omega_0) z]}$, $\left|A\right| = \sqrt{P}$

where "ω_0" may be chosen as the center frequency of the DWDM band.

DWDM signal can now be expressed as

$$A(z,t) = \frac{1}{2}\left[\sum_{m=1}^{M} B_m(z,t) e^{jC_m} + c.c.\right] \tag{D.4}$$

with $B_m(z,t) = \sqrt{P_m} I_m(t) e^{-\frac{\alpha}{2}z}$ where $\int_{-\infty}^{+\infty} I_m(t) dt = 1$ is the input pulse shape

$$C_m = \omega_m t - \left[\beta_{0,m} + \omega\beta_{1,m} + \frac{1}{2}\omega^2\beta_{2,m} + \cdots\right] z \tag{D.5}$$

$$\omega_m \to \omega_m - \omega_0, \qquad \beta_{i,m} = \left.\frac{\partial^i \beta_m}{\partial \omega^i}\right|_{\omega_0}, \qquad \beta_{0,m} = \beta(\omega_m) - \beta(\omega_0) \tag{D.6}$$

The time dependence of nonlinear polarization component is modelled as an instantaneous process. It is also assumed the contribution of "$\beta_{1,m}$, $\beta_{2,m}$" are negligible when calculating Kerr type nonlinear effects.

Then writing G_m for $G_m = \sqrt{P} I(t) e^{-\frac{\alpha}{2} z} e^{j\phi_m}$ and Ψ_m for $\Psi_m = \omega_m t - \beta_m z$ where $\beta_m = \beta_{0,m}$ the DWDM signal can be expressed simply as

$$A(z,t) = \frac{1}{2}\left[\sum_{i=1}^{M} G_m e^{j\Psi_m} + c.c.\right] \tag{D.7}$$

Full Width at Half Maximum of Gaussian Pulse

To define the pulse width for an arbitrary pulse, the full width at half maximum (FWHM) intensity points are used. Using the FWHM as a specification allows a single number to unambiguously describe the properties of the Gaussian envelope, Fig. D.2. Assuming a Gaussian pulse shape in time, and writing the pulsed electric field centered at ω_0 as

$$E(t) = E_0 e^{-\left[\frac{t}{\tau}\right]^2} e^{-i\omega_0 t} \tag{D.8}$$

Detectors respond to intensity, which is defined as

$$I(t) = E^*(t) E(t) \tag{D.9}$$

$$= E_0^2 e^{-\frac{2t^2}{\tau^2}} \tag{D.10}$$

When the intensity is at half its maximum value,

$$\frac{1}{2} = e^{-\left[\frac{2T^2}{\tau^2}\right]} \tag{D.11}$$

$$-\ln\left(\frac{1}{2}\right) = \frac{2T^2}{\tau^2} \tag{D.12}$$

$$T = \tau\sqrt{\frac{\ln(2)}{2}} \tag{D.13}$$

$$FWHM = 2T \tag{D.14}$$

$$= \tau\sqrt{2\ln(2)} \tag{D.15}$$

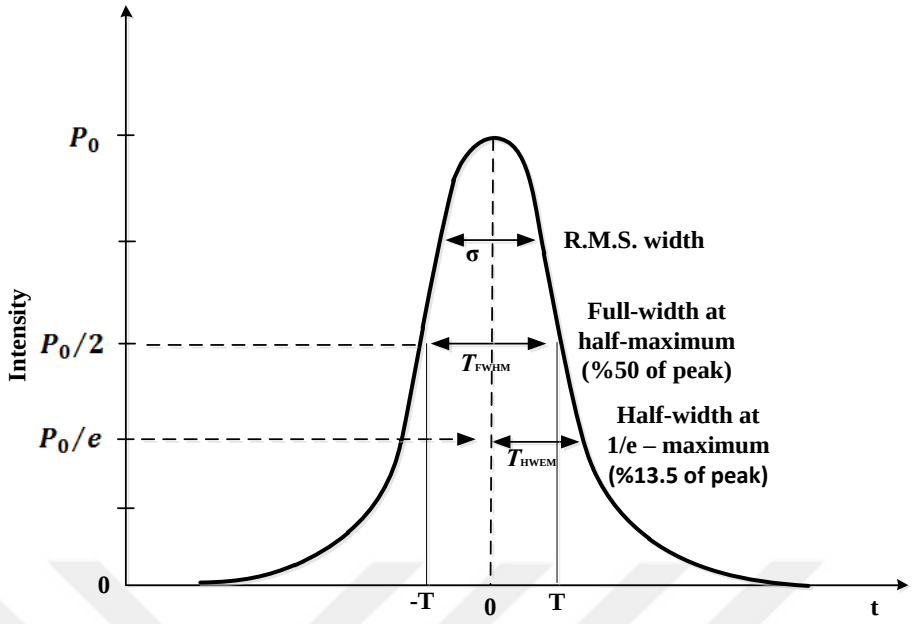

Figure D.2: Normalized Gaussian beam Intensity as a function of t [3].

where E(t) = pulse's electric field amplitude (voltage), V / m

P_0 = pulse's optical peak power, W

t = time, s

σ = RMS width of the pulse's optical power, s

T_{HWEM} = half pulse width at $1/e$ optical power point, s

T_{FWHM} = full pulse width at half maximum optical power point (-3 dB), s

Full width at half maximum. FWHM=2T

The spectral field is given by the Fourier transform of the temporal field in Equation D.8. Note that it is the fields that are transformed, and not the intensities.

$$E(\omega) = \int_{-\infty}^{+\infty} E(t)e^{+i\omega t}dt = \sqrt{\pi}E_0\tau e^{-\left[\frac{(\omega-\omega_0)\tau}{2}\right]^2} \tag{D.16}$$

Comparison with the Equations D.8 and D.15 shows that

$$\text{Spectral Width} = \frac{2}{\tau}\sqrt{2\ln(2)} \tag{D.17}$$

$$E(t) = \sqrt{P_o}\exp\left(-\frac{1}{2}\left(\frac{t}{T_{HWEM}}\right)^2\right) \tag{D.18}$$

$$P(t) = P_0\exp\left(-\left(\frac{t}{T_{HWEM}}\right)^2\right) \tag{D.19}$$

$$\sigma = \frac{1}{\sqrt{2}}T_{HWEM} \tag{D.20}$$

$$\sigma = \frac{1}{2\sqrt{2\ln 2}}T_{FWHM} \tag{D.21}$$

$$T_{FWHM} = 2\sqrt{2\ln 2}\ T_{HWEM} \tag{D.22}$$

APPENDIX- E

Derivation of phase-mismatch parameter

Phase mismatch factor is estimated by expanding the propagation constant in Taylor series around $\omega = \omega_m = 2\pi c/\lambda_m$ as follows:

$$\beta(\omega) = \beta(\omega_m) + \beta_1(\omega - \omega_m) + \frac{1}{2}\beta_2(\omega - \omega_m)^2 + \cdots \tag{E.1}$$

where $\beta(\omega_m) = \beta_0$ is propagation parameter, β_1 is the inverse of the group velocity, β_2 is the group velocity dispersion (pulse propagation parameter) respectively.

Using $\beta_2 = -\frac{2\pi c}{\lambda^2} D$, one can write

$$\beta(\omega) = \frac{\omega_m}{v_p} + \frac{\omega - \omega_m}{v_g} + (\omega - \omega_m)^2 \frac{\lambda_m^2 D_c}{4\pi c} + (\omega - \omega_m)^3 \frac{\lambda_m^4}{24\pi^2 c^2} \frac{dD_c}{d\lambda} \tag{E.2}$$

Therefore, $\Delta\beta = \beta_i + \beta_j - \beta_k - \beta_{ijk}$ can be deduced as:

$$\Delta\beta = \beta_{ijk} + \beta_k - \beta_i - \beta_j \tag{E.3}$$

$$\Delta\beta = (\omega_k - \omega_i)(\omega_k - \omega_j)\frac{\lambda_m^2 D_c}{2\pi c} + (\omega_k - \omega_i)(\omega_k - \omega_j)(\omega_i + \omega_j - 2\omega_m)\frac{\lambda_m^4}{8\pi^2 c^2}\frac{dD_c}{d\lambda} \tag{E.4}$$

If center wavelength is far from the zero-dispersion wavelength the last term can be negelected and phase mismatch becomes

$$\Delta\beta = (\omega_k - \omega_i)(\omega_k - \omega_j)\frac{\lambda_m^2 D_c}{2\pi c} = (f_k - f_i)(f_k - f_j)\frac{2\pi\lambda_m^2 D_c}{c} \tag{E.5}$$

If the center wavelength is locate near the zero-dispersion wavelength, then $Dc \approx 0$ and the last term representing higher order dispersion dominates:

$$\begin{aligned}\Delta\beta &= (\omega_k - \omega_i)(\omega_k - \omega_j)(\omega_i + \omega_j - 2\omega_0)\frac{\lambda_m^4}{8\pi^2 c^2}\frac{dDc}{d\lambda} \\ &= (f_k - f_i)(f_k - f_j)(f_i + f_j - 2f_0)\frac{\pi\lambda_m^4}{c^2}\frac{dDc}{d\lambda}\end{aligned} \tag{E.6}$$

APPENDIX-F

Matlab code & GUI

MATLAB CODE:

```
close all; clear all; clc;
i=sqrt(-1);c=3e8;
P0=0.001; % W
alfadB=0; % dB/km
D=17; % ps/nm*km
lambda=1550; %  nm
n2=3.2e-16; % cm^2/W
Aef=50; % um^2
z=50; % km
dz=0.25; % 0.1 - 1 km
T0=50; %HWEM  A=A0*1/e
C=0; %chirp
m=1; %deg of gauss
N=1024; %
tau=400; %
%--------------------------------------------------------------------------
beta2=-D*1e-24*((lambda)^2)/(2*pi*c);% s^2/m
gamma=(2*pi*n2*1e17)/(lambda*Aef); %1/m.W
BW=(1/tau)*1000;  %GHz
Bit=tau/(2*T0);
BR=(BW)*Bit;
T0=(T0)*1e-12;
Ld=(T0^2)/abs(beta2);
save initials2.mat Ld beta2 BW BR
h=z/dz;
dz=dz*1000;                                %km -> m
alfa=(1*alfadB/4.343)/1000;                % 1/m
t=-(tau/2)*1e-12:(tau*1e-12)/(N-1):(tau/2)*1e-12;          %
dt=(tau*1e-12)/(N-1);
```

```
A=sqrt(P0)*exp((-(1+i*C)/2)*(t/T0).^(2*m)); % Electric Field Amplitude (voltage, V/m)
I=(abs(A)).^2;                          %Intensity Optical Intensity
plot(t*1e12,I/P0,'k','LineWidth',1.2);   %Normalized Intensity
xlabel('Time [ps]');
ylabel('Normalized Intensity');
grid on;hold on;
l=length(A);
dw=2*pi*1/(dt*l);
w=(-1*l/2:1:l/2-1)*dw;
w=fftshift(w);
freq_A0=fft(A);
for k=1:h,
   freq_A1=freq_A0.*exp(-(alfa/2)*(dz/2)+i*w.^2*(beta2/2)*(dz/2));
   time_A1=ifft(freq_A1);
   time_A2=time_A1.*exp(i*gamma*(abs(A)).^2*dz);
   freq_A2=fft(time_A2);
   freq_A0=freq_A2.*exp(-(alfa/2)*(dz/2)+i*w.^2*(beta2/2)*(dz/2));
end;
 A=ifft(freq_A0);
 title('\it{Input and Output Pulse Shape}','FontSize',12)
 plot(t*1e12,(abs(A)).^2/P0,'r-','LineWidth',1.2);  %/sqrt(P0)
 Pout=max(abs(A)).^2;
 save initials2.mat Ld beta2 BW BR Pout
 legend('input','output');
```

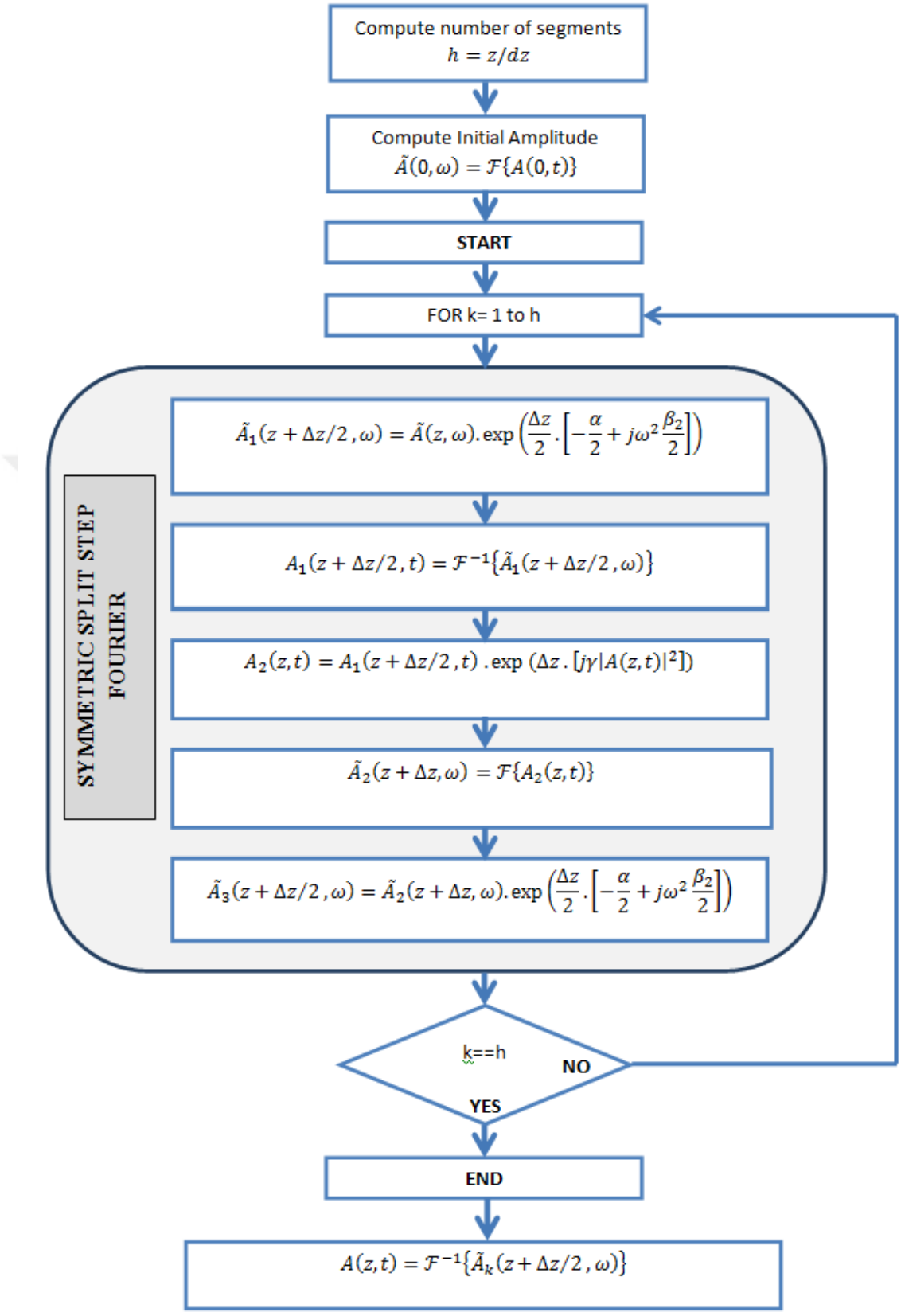

Figure F.1: Flow diagram of the symmetric Split-Step Fourier Method for solving the Nonlinear-Schrödinger Equation.

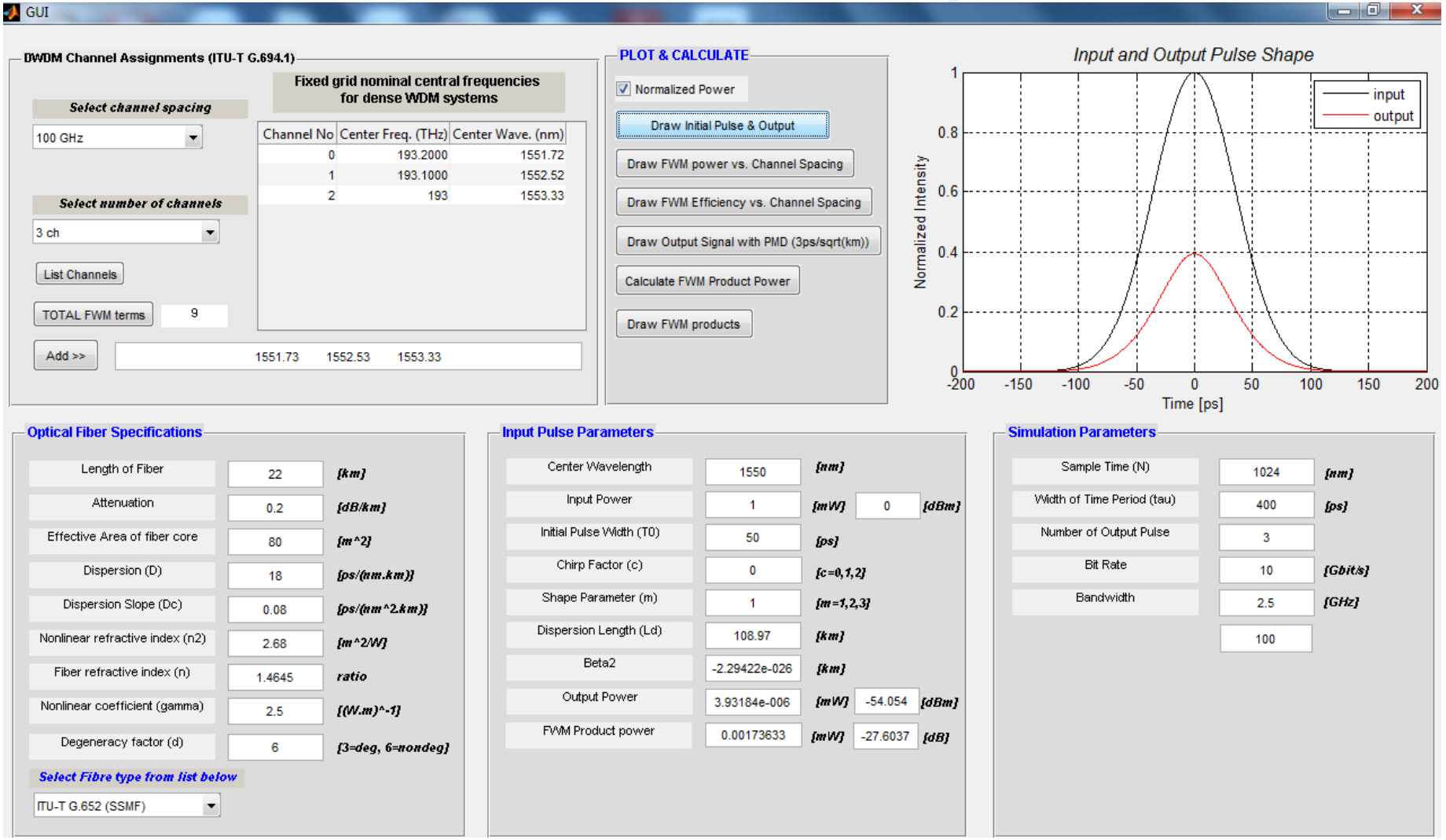
GUI
DWDM Channel Assignments (ITU-T G.694.1)
Fixed grid nominal central frequencies for dense WDM systems
Select channel spacing
100 GHz
Select number of channels
3 ch
List Channels
TOTAL FWM terms
9
Add >>
1551.73 1552.53 1553.33
Channel No | Center Freq. (THz) | Center Wave. (nm)
0 193.2000 1551.72
1 193.1000 1552.52
2 193 1553.33
PLOT & CALCULATE
Normalized Power
Draw Initial Pulse & Output
Draw FWM power vs. Channel Spacing
Draw FWM Efficiency vs. Channel Spacing
Draw Output Signal with PMD (3ps/sqrt(km))
Calculate FWM Product Power
Draw FWM products
Input and Output Pulse Shape
input
output
Normalized Intensity
Time [ps]
Optical Fiber Specifications
Length of Fiber 22 {km}
Attenuation 0.2 {dB/km}
Effective Area of fiber core 80 {m^2}
Dispersion (D) 18 {ps/(nm.km)}
Dispersion Slope (Dc) 0.08 {ps/(nm^2.km)}
Nonlinear refractive index (n2) 2.68 {m^2/W}
Fiber refractive index (n) 1.4645 ratio
Nonlinear coefficient (gamma) 2.5 {(W.m)^-1}
Degeneracy factor (d) 6 {3=deg, 6=nondeg}
Select Fibre type from list below
ITU-T G.652 (SSMF)
Input Pulse Parameters
Center Wavelength 1550 {nm}
Input Power 1 {mW} 0 {dBm}
Initial Pulse Width (T0) 50 {ps}
Chirp Factor (c) 0 {c=0,1,2}
Shape Parameter (m) 1 {m=1,2,3}
Dispersion Length (Ld) 108.97 {km}
Beta2 -2.29422e-026 {km}
Output Power 3.93184e-006 {mW} -54.054 {dBm}
FWM Product power 0.00173633 {mW} -27.6037 {dB}
Simulation Parameters
Sample Time (N) 1024 {nm}
Width of Time Period (tau) 400 {ps}
Number of Output Pulse 3
Bit Rate 10 {Gbit/s}
Bandwidth 2.5 {GHz}
100

APPENDIX-G

ITU-T DWDM FREQUENCY GRID OF 100 GHZ 0.8 nm

ITU Grid Channels (100 GHz Spacing)					
Channel	Frequency (GHz)	Wavelength (nm)	Channel	Frequency (GHz)	Wavelength (nm)
1	190,100	1577.03	38	193,800	1546.92
2	190,200	1576.20	39	193,900	1546.12
3	190,300	1575.37	40	194,000	1545.32
4	190,400	1574.54	41	194,100	1544.53
5	190,500	1573.71	42	194,200	1543.73
6	190,600	1572.89	43	194,300	1542.94
7	190,700	1572.06	44	194,400	1542.14
8	190,800	1571.24	45	194,500	1541.35
9	190,900	1570.42	46	194,600	1540.56
10	191,000	1569.59	47	194,700	1539.77
11	191,100	1568.77	48	194,800	1538.98
12	191,200	1567.95	49	194,900	1538.19
13	191,300	1567.13	50	195,000	1537.40
14	191,400	1566.31	51	195,100	1536.61
15	191,500	1565.50	52	195,200	1535.82
16	191,600	1564.68	53	195,300	1535.04
17	191,700	1563.86	54	195,400	1534.25
18	191,800	1563.05	55	195,500	1533.47
19	191,900	1562.23	56	195,600	1532.68
20	192,000	1561.42	57	195,700	1531.90
21	192,100	1560.61	58	195,800	1531.12
22	192,200	1559.79	59	195,900	1530.33
23	192,300	1558.98	60	196,000	1529.55
24	192,400	1558.17	61	196,100	1528.77
25	192,500	1557.36	62	196,200	1527.99
26	192,600	1556.55	63	196,300	1527.22
27	192,700	1555.75	64	196,400	1526.44
28	192,800	1554.94	65	196,500	1525.66
29	192,900	1554.13	66	196,600	1524.89
30	193,000	1553.33	67	196,700	1524.11
31	193,100	1552.52	68	196,800	1523.34
32	193,200	1551.72	69	196,900	1522.56
33	193,300	1550.92	70	197,000	1521.79
34	193,400	1550.12	71	197,100	1521.02
35	193,500	1549.32	72	197,200	1520.25
36	193,600	1548.51	73	197,300	1519.48
37	193,700	1547.72			

APPENDIX-H

Optical Data Transmission Rates

For many transmission systems, it is mandatory to multiplex of numerous channels to fully utilize system capacity. *Time-division multiplexing (TDM)* and *frequency-division multiplexing (FDM)* are two powerful techniques to perform this in both electrical and optical domains. Optical FDM is often referred to as WDM.

Currently, widely used transmission and multiplexing standard for high-speed signals within the carrier infrastructure in North America is *SONET (Synchronous Optical Network).*

SDH (Synchronous Digital Hierarchy) is the another similarly related standard which has been developed for Europe and Japan. (Table H.1.)

Table H.1: Transmission data rates for SONET/SDH.

SONET	***SDH***	***Bit Rate (Mb/s)***	***Channels***
OC-1 (STS-1)		51.84	672
OC-3 (STS-3)	STM-1	155.52	2016
OC-12 (STS-12)	STM-4	622.08	8064
OC-24 (STS-24)		1244.16	16128
OC-48 (STS-48)	STM-16	2488.32	32256
OC-192 (STS-192)	STM-64	9953.28	129024
OC-768 (STS-768)	STM-256	39814.32	516096

Table H.2: OTN line rates compared with SONET/SDH line rates.

OTN (G.709)	***Line Rates***	***SONET/SDH***	***Line Rates***
OTU-1	2.666 Gb/s	STS-48 / STM-16	2.488 Gb/s
OTU-2	10.709 Gb/s	STS - 192 / STM-64	9.953 Gb/s
OTU-3	43.018 Gb/s	STS-768 / STM-128	39.813 Gb/s

The *Optical Transport Network (OTN),* which is referred to ITU standard of G.709, was designed to transport data packet traffic such as IP and Ethernet over fiber optics, as well as legacy traffic and in particular SONET/SDH. In OTN technology, client signal is wrapped in overhead information for operations, administration, and management. Used line rates OTU1, OTU2, and OTU3, are shown in Table H.2. which are build on SONET/SDH concepts [13].

CURRICULUM VITAE

Name Surname: Onur Erkan

Place and Date of Birth: İstanbul, 1983

Address: Büyükdere Cad. No:255 Nurol Plaza Maslak-Şişli/İST

E-mail: onurerkan@gmail.com

Undergraduate: Yıldız Technical University, Electrical Engineering

Professional Experiences: Fiber Optics and Transmission Network Planning Executive

Vodafone Turkey